Mark, Thesis 11/9/01 11:28 AM Page 271

# INTRAOCULAR RETINAL PROSTHESIS

BY *Mark S. Humayun, MD, PhD*

**ABSTRACT**

*Purpose*: An electronic implant that can bypass the damaged photoreceptors and electrically stimulate the remaining retinal neurons to restore useful vision has been proposed. A number of key questions remain to make this approach feasible. The goal of this thesis is to address the following 2 specific null hypotheses: (1) Stimulus parameters make no difference in the electrically elicited retinal responses. (2) Just as we have millions of photoreceptors, so it will take a device that can generate millions of pixels/light points to create useful vision.

*Methods*: For electrophysiologic experiments, 2 different setups were used. In the first setup, charge-balanced pulses were delivered to the retinal surface via electrodes inserted through an open sky approach in normal or blind retinal degenerate (rd) mice. In the second setup, the rabbit retina was removed under red light conditions from an enucleated eye and then maintained in a chamber while being superfused with oxygenated, heated Ames media. In both setups, stimulating electrodes and recording electrodes were positioned on the retinal surface to evaluate the effect of varying stimulation parameters on the orthodromic retinal responses (ie, recording electrode placed between stimulating electrodes and optic nerve head).

For psychophysical experiments, visual images were divided into pixels of light that could be projected in a pattern on the retina in up to 8 sighted volunteers. Subjects were asked to perform various tasks ranging from reading and face recognition to various activities of daily living.

*Results*: Electrophysiologic experiments: In a normal mouse, a single cycle of a 1-kHz sine wave was significantly more efficient than a 1-kHz square wave ($P < .05$), but no such difference was noted in either of the 8- or 16-week-old rd mouse groups (8-week-old, $P = .426$; 16-week-old, $P = .078$). Charge threshold was significantly higher in 16-week-old rd mouse versus both 8-week-old rd and normal mouse for every stimulus duration ($P < .05$). In all groups, short duration pulses (40, 80, and 120 μs) were more efficient in terms of total charge (the product of pulse amplitude and pulse duration) than longer (500 and 1,000 μs) pulses ($P < .05$). In all groups, applying a pulse train did not lead to more efficient charge usage ($P < .05$).

Psychophysical experiments: In high-contrast tests, facial recognition rates of over 75% were achieved for all subjects with dot sizes of up to 31.5 minutes of arc when using a 25 x 25 grid with 4.5 arc minute gaps, a 30% dropout rate, and 6 gray levels. Even with a 4 x 4 array of pixels, some subjects were able to accurately describe 2 of the objects. Subjects who were able to read the 4-pixel letter height sentences (on the 6 x 10 and 16 x 16 array) seemed to have a good scanning technique. Scanning at the proper velocity tends to bring out more contrast in the lettering. The reading speed for the 72-point font is a bit slower than for the next smaller font. This may be due to the limited number of letters (3) visible in the window with this large font.

Conclusions: Specific parameters needed to stimulate the retina were identified. Delineating the optimum parameters will decrease the current requirements. Psychophysical tests show that with limited pixels and image processing, useful vision is possible. Both these findings should greatly simplify the engineering of an electronic retinal prosthesis.

*Tr Am Ophth Soc* 2001;99:271-300

## INTRODUCTION

### 1. HISTORICAL OVERVIEW AND CURRENT APPROACHES

Blindness afflicts more than 1 million Americans, and approximately 10% have no light perception.[1] A number of approaches, including gene and drug therapies, are currently being pursued in the hope of preventing blindness.[2,3] Nevertheless, once vision is totally lost, only 2 of the existing approaches show promise for reversing the ailment: retinal transplantation[3,4] and bioelectronic visual prosthesis.

During the 18th century, scientists understood that electricity could elicit a response in biological tissues.[5,6] The era of electronic implants was ushered in by both cardiac pacemakers and cochlear implants.[7,8] Since then, along with the development of a visual prosthesis, electrical stimulation has been proposed to restore limb function

*From the Retina Institute, Doheny Eye Institute, Keck School of Medicine of USC, Los Angeles, California. Supported by grant EY 11888 from the National Eye Institute, BES 9810914 from the National Science Foundation, and EY 12893 from the National Institutes of Health.

Mark, Thesis 11/9/01 11:28 AM Page 272



in paraplegics and quadriplegics[9-11] as well as to suppress intractable pain[12] and Parkinsonian tremor.[13]

*1.1 Cortical Prosthesis*

Work toward a visual prosthesis started with electrical stimulation of the visual cortex. Direct electrical stimulation of the cortical surface under local anesthesia of a sighted human subject resulted in seeing a spot of light (phosphene). The position of the light in space corresponded correctly to the stimulated anatomical region.[14] Subsequently, similar results were obtained in blind patients.[15-17] In another experiment, electrodes were implanted over a period of 3 to 10 weeks on the occipital cortex of 3 blind patients. Two of these patients were able to locate a light source by scanning the visual field with a photocell, the output of which electrically stimulated the cortex via a wire passing through the scalp and skull.[18]

A key experiment in this field was performed when 80 electrodes were implanted on the visual cortical surface of a 52-year-old nurse blind from bilateral severe glaucoma and retinal detachment in the left eye. Wires through a burr hole connected each electrode to a radio receiver screwed to the outer bony surface. An oscillator coil was placed above a given receiver in order to activate the receiver via radio frequency and stimulate the cortex. With this system, the patient was able to see light points in 40 different positions of the visual field, demonstrating that half of the implanted electrodes were functional. This experiment showed that a chronically activated electrical stimulation device could be safe.[19] A second implantation by the same group was performed in a blind 64-year-old patient with retinitis pigmentosa (RP). He was able to read random letters at 8.5 characters per minute.[20]

In spite of the ability to induce phosphenes, there were many difficulties to overcome. These included phosphene flickering during surface stimulation;[19,21,23,24] the need for high currents and large electrodes to induce phosphenes;[24] and interactions between phosphenes when electrodes were placed less than 2.4 mm apart. The same stimulating electrode inducing multiple phosphenes and those produced were inconsistent. Occasionally, pain was induced owing to meningeal stimulation. Other drawbacks included limited two-point discrimination, local heating and electrolysis,[25] and phosphene persistence following cessation of electrical stimulation.[26]

In spite of all the shortcomings, efforts continued and other 64-channel platinum disc electrode arrays were implanted on the occipital cortical surface of blind patients.[21;27-29] The prosthesis allowed blind patients to read "phosphene Braille" 2 to 3 times faster than tactile Braille and to recognize 6-inch characters at 5 feet (approximately 20/1200 visual acuity).[30] It was also found that phosphene brightness was a logarithmic function of stimulating current amplitude.[27]

However, the need for smaller electrodes and more localized phosphenes forced the development of intracortical electrodes.[26,31-36] During a planned neurosurgical procedure to excise epileptic foci of the brain under local anesthesia, 1 group inserted 37.5 mm-diameter iridium microelectrodes into the occipital cortex of these patients. Stimulation was performed with both surface and intracortical electrodes. Both methods elicited phosphenes, but the stimulus current threshold for intracortical microstimulation was 10 to 100 times lower than that for stimulation using surface electrodes.[26] Based on intracortical electrodes, a new cortical prosthesis with 38 microelectrodes was implanted in an area 40.8 x 19.2 mm in the visual cortex of a 42-year-old patient totally blind for 22 years due to glaucoma. The electrodes were implanted for a period of 4 months, and this experiment showed that despite being blind for many years, the subject was able to perceive phosphenes at a predictable and reproducible location in the visual space.[32] It was also demonstrated that simple patterned perceptions could be evoked by electrical stimulation via small groups of these microelectrodes. Electrodes spaced as close as 500 mm apart generated separate phosphenes, and at levels near threshold, the phosphenes usually had colors.

Undoubtedly, the lower current threshold of the intracortical microstimulation, the predictable forms of generated phosphenes, the absence of flicker phenomenon, reduction of phosphene interactions, the opportunity to increase the number of electrodes, the power requirement improvement, and the current per microelectrode reduction are the main advantages of the intracortical microstimulation approach.[26,32] Because of these advantages, all major efforts investigating the development of a visual cortical prosthesis have abandoned the use of surface electrodes and are developing intracortical microstimulating electrodes.

There are advantages and disadvantages that are associated with the cortical stimulation approach in general. The skull will protect both the electronics and the electrode array, and a cortical prosthesis will bypass all diseased neurons distal to the primary visual cortex. By doing so, it has the potential to restore vision to the largest number of blind patients. However, spatial organization is more complex at the cortical level and 2 adjacent cortical loci do not necessarily map out to 2 adjacent areas in space, so that patterned electrical stimulation may not produce the desired patterned perception. In addition, the convoluted cortical surface makes it difficult for implantation, and surgical complications can have devastating results, including death.

*1.2 Retinal Prostheses*

During the early 1970s, it became clear that blind humans

Mark, Thesis 11/9/01 11:28 AM Page 273



can also perceive electrically elicited phosphenes in response to ocular stimulation, with a contact lens as a stimulating electrode.[37-39] When obtainable, these electrically elicited responses indicated the presence of at least some functioning inner retinal cells. Since a number of blinding retinal diseases are due predominantly to degeneration of outer retina or photoreceptors,[40-42] the idea of stimulating the remaining inner retina has been proposed (Figs 1 and 2).

Progress in the field of neural prostheses has converged with advances in retinal surgery to enable the development of an implantable retinal prosthesis. At present, this implant is aimed at patients blinded primarily by photoreceptor loss such as RP and some forms of age-related macular degeneration (AMD). These 2 degenerations are common and account for a significant percent of the blind population. The incidence of RP is 1 per 4,000 live births, and there are approximately 1.5 million people affected worldwide, making RP the leading cause of inherited blindness.[2] AMD is the main cause of visual loss among adults older than 65 years of age in Western countries. Annually, there are approximately 700,000 new patients in the United States who lose vision on account of this illness, and 10% of these become legally blind each year.[43]

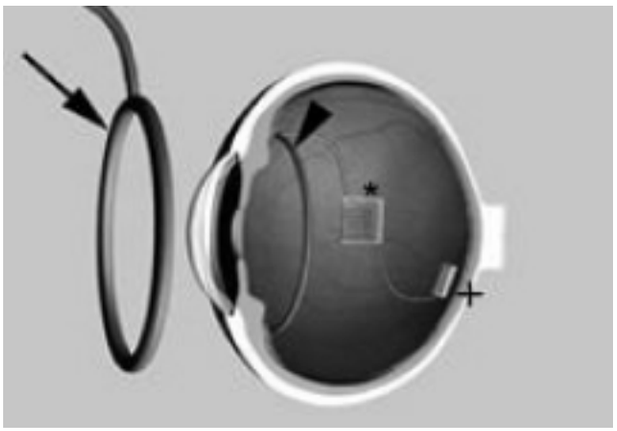

**FIGURE 1**

Intraocular retinal prosthesis. Both power and data are delivered via an inductive link. Camera (not shown) and transmitter coil are in glass frame, and receiver coil is placed in sulcus. Microelectronics are positioned in vitreous so as to reduce risk of harming retina through either mechanical or electrical damage. Only a delicate electrode array is affixed to retinal to transmit electrical pulses. Primary (arrow) and secondary (arrowhead) coils. Asterisk denotes a rectifier and regulator, a retinal stimulator with a telemetry protocol decoder, and stimulus signal generator. Plus symbol denotes an electrode array.

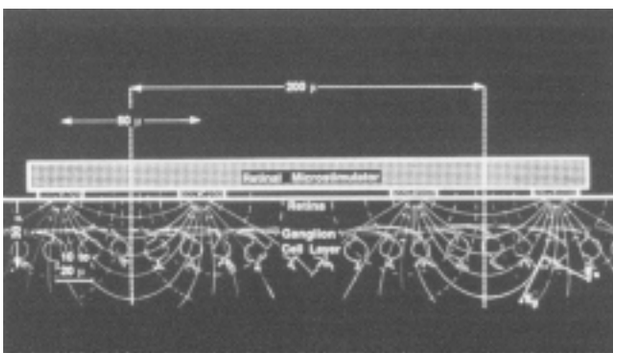


**FIGURE 2**

Schematic of epiretinal electrode array part of intraocular retinal prosthesis. By passing electrical current between electrodes, electronic implant will excite remaining underlying retinal neurons.

Postmortem morphometric analysis of the retina of patients with RP has shown that many more inner nuclear layer cells (bipolar cells and others, 78.4%) are retained compared to outer nuclear layer (photoreceptors, 4.9%) and ganglion cell layer (29.7%).[40-42] Similar results have been found in patients with AMD.[44] Given that there is limited transsynaptic neuronal degeneration, it does seem feasible to stimulate the remaining retinal neurons.

Currently, several groups have been developing retinal and optic nerve prostheses.[45-53] These groups can be classified according to the location of their device: on the retinal surface (epiretinal), in the subretinal space, or around the optic nerve (Fig 3).

To examine if these remaining retinal neurons could be electrically excited in a manner that might restore useful vision, intraocular retinal stimulation studies were performed. Prior to the surgical procedure, patients had to pass a screening test, which grossly tested the inner retinal function. In this screening test, in an outpatient clinic setting, they had to perceive light in response to electrical stimulus delivered by a contact lens connected to a computer (electrical evoked response). Following this initial screening, the surgery involved a three-port pars plana vitreoretinal procedure with subconjunctival anesthesia placed only over the sclerotomies in order to avoid

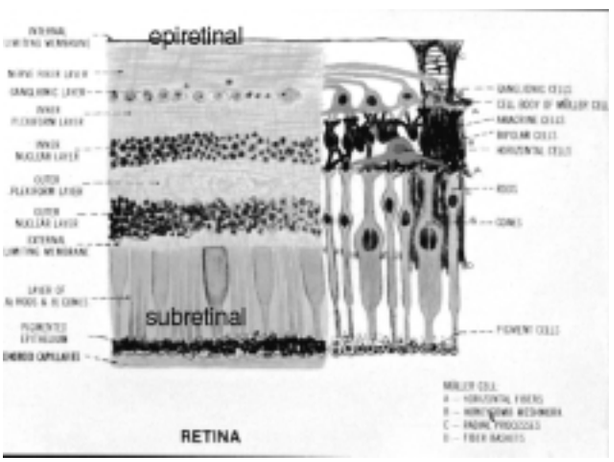


**FIGURE 3**

Retinal cytoarchitecture. Text shows placement of epiretinal and subretinal devices.

Mark, Thesis 11/9/01 11:28 AM Page 274



disrupting the optic nerve function. Different types of handheld stimulating electrodes were positioned on the retinal surface (ie, almost touching the internal limiting lamina). Computer-generated current pulses were then delivered through these electrodes, and the patients were then asked to tell the surgeons about their visual perceptions.

Focal electrical stimulation elicited "phosphenes" in all the patients, and 4 or 5 patients were able to describe spatial and temporal aspects of the stimuli. The resolution was estimated to be 4.5 per 200, consistent with crude ambulatory vision.[54]

Recently, epiretinal electric stimulation was further tested in nine other patients with RP or AMD.[47] Two patients were tested with an electrode array consisting of 3 x 3, 5 x 5, or 3 x 7 electrodes. Seven other subjects were tested with simple devices consisting of 3 platinum electrodes packaged as a surgical instrument in a handpiece. The study showed that in the patients with RP, the electrical stimulation threshold was dependent on the electrode's location (ie, the macular region required higher threshold currents than the peripheral retina to elicit visual perceptions). Also, patients with less advanced RP or AMD required lower threshold currents than those with more advanced disease. These findings are important because lower thresholds would allow for smaller and therefore higher density of electrodes and hence greater resolution. Lower threshold values in healthier retinas were later confirmed by other experiments.[55-58]

Perhaps the most important result of these human studies was the patients' ability to use the pattern electrical stimulation to recognize shapes and forms. Patients were able to identify crude forms such as a single letter or a box shape during the short period of electrical stimulation testing. When the electrical stimulation ended, there was no persistence of the image. Later, another group also confirmed some of these results in healthy retina of a sighted volunteer.[58] Other important psychophysical perceptions in this study included flicker fusion (at a frequency of 40 to 50 Hz) and different color perceptions.[47]

Thus far, the results mentioned have all been from the epiretinal electrical stimulation. By having a significant portion of the electronics wearable at the eyeglass frame rather than implanted, the epiretinal implantation minimizes the risk of failure and optimizes the ease of replacement or upgrading the electronics. Additionally, a majority of the implanted intraocular electronics could be placed in the vitreous cavity, a naturally existing fluid-filled space, which greatly helps in dissipating heat generated by the electronics.[50,59,60] However, an epiretinal prosthesis will be exposed to ocular rotational movements, making the need for a nontraumatic yet sturdy attachment method paramount. Also, by physically being closer to the retinal ganglion cells (RGCs), it may be more difficult to stimulate bipolar cells, and therefore one may lose the visual processing that takes place in this layer.

The subretinal approach has equally made great strides. Recently, a phase I clinical trial of subretinal visual prosthesis implantation in 3 human subjects was announced. Measuring 2 mm in diameter and 0.25 mm thick, this retinal prosthesis contains 3,500 solar cells that generate power from light that enters the eye.[61] The subretinal positioning of the retinal prosthesis has the advantage of placing the stimulating electrodes closer to the bipolar cells, which may also permit lower stimulus thresholds.[48,49,62-65] However, the placement of any object between the choroid and the retina can be more disruptive to the nutritional supply of the retina derived from the choroid.[48] Another drawback of this method is the limited amount of light that can reach the array coupled with the inefficiency of modern-day photovoltaic or solar cells. This translates into using a very bright and nonfeasible image intensifier (10 suns) in order for the stimulator chip to generate the level of currents that have resulted in visual perceptions in the blind. Regardless of whether the implant is positioned on the epiretinal or subretinal surface, there are distinct advantages and inherent disadvantages associated with these intraocular retinal stimulation approaches. The advantages include the ability to use existing physiologic optics and retinotopic organization of the eye in addition to the natural processing ability along the proximal visual pathways. Furthermore, the vitreous cavity fluid can be utilized as a heat sink, and the prosthesis could be visualized by dilating the pupil in an outpatient setting. Less surgical morbidity and mortality are expected in comparison to any of the cortical prostheses implantation methods. The disadvantages of the retinal stimulation approach include the following: possible disruption of retinotopic organization due to nonselective stimulation of ganglion cells' axons; possible difficulties in chronic attachment of a device to the retina; inability to properly encode many properties of the visible light (eg, color, intensity) that the retina naturally does so well; and the fact that this approach is limited to outer retinal pathologies.

### *1.3 Optic Nerve Prosthesis*

Investigators have also stimulated the optic nerve.[66,52,67] In spite of the relative ease of reaching the optic nerve during surgery, the high density of the axons (1.2 million within an approximately 2 mm-diameter cylindrical structure) could make it difficult to achieve focal stimulation and detailed perceptions. In addition, any surgical approach to the optic nerve requires dissection of the dura and can have harmful side effects. Similar to the retinal prosthesis approach, optic nerve stimulation requires intact RGCs and is limited to outer retinal pathologies.

Mark, Thesis 11/9/01 11:28 AM Page 275



Recently, 1 of the groups chronically implanted a self-sizing spiral cuff electrode with 4 contacts around the optic nerve of a 59-year-old blind patient with RP. Electrical stimuli applied to the optic nerve produced localized, often colored phosphenes that were broadly distributed throughout the visual field and were reliably reinduced 118 days after surgery. Changing the pulse duration (PD) or pulse frequency could vary phosphene brightness.[52]

Yet another approach, a hybrid retinal implant, proposes to develop an integrated circuit, which would include both electronic and cellular components. The electronics will perform image recognition, and the neurons on the device will extend their axons to synapse with the lateral geniculate body and thus create the device-CNS interface and restore vision.[53,68] The advantage of this approach is to be able to reconstruct an eye with total or inner retinal degeneration. Disadvantages include difficulties in precisely directing axons to the lateral geniculate body, developing the interface between the electronics and neurons, and an environment to enable survival of the cellular components while being housed in microelectronics.

*1.4 Sensory Substitution Devices*

As an alternative to direct stimulation of the visual system neurons, several other approaches have attempted to convert visual information into vibrotactile or auditory signals (ie, sensory substitution devices[69,70]). The distinct advantage of these approaches is that the device is wearable and not implantable. However, these devices have never reached widespread acceptance because they do not restore the sensation of vision, have low resolution, occupy another sensory modality, can evoke pain, and can have a prolonged learning period.

## 2. BIOCOMPATIBILITY

Biocompatibility issues are of paramount concern with any implantable device. The implant has to be constructed and implanted in a manner so as not to damage the tissue but also so the implant will function reliably over many decades. In the case of an electronic retinal prosthesis, there are both mechanical and electrical concerns.

*2.1 Mechanical Biocompatibility*

2.1.1 *Infection and inflammation*. Despite the fact that the CNS and the eye have been described as immunologically or partially immunologically privileged sites,[71,72] the course of inflammation is identical to that occurring elsewhere in the body once an incitement of inflammation has occurred.[73] Mere surgical manipulation, as well as infection, biodegradation, or the release of toxic substances from the implant, can provoke the inflammatory response. Bacterial infections are often delayed and appear to be due in part to the host's inability to respond properly to infections. Their origin is frequently distant infected sites in the body or skin flora.[74] Less often, the origin is infected implants and surgical and nursing staff.

2.1.1.1 *Cortical implantation*. The biocompatibility of various chronic intracortical stimulating arrays was examined. Preliminary experiments of chronic implantation of stimulating devices over the cortex revealed a fibrous membrane covering the surface of every implant that was examined 6 weeks or more after insertion. These membranes had little effect on threshold for stimulation.[19] There was only 1 report on the need to remove a chronic device from the cortical surface of a patient because of a blood-borne infection.[30]

2.1.1.2 *Retinal prosthesis*. The field of retinal prostheses is relatively new, and few reports on chronic implantation and adverse reaction are available. In the few experiments done, some used only sham devices with no electrical stimulation in order to examine mechanical biocompatibility. In 1 such study, performed in 4 dogs, no retinal detachment occurred and only retinal pigment epithelium (RPE) changes were noted near the retinal tacks, which were used for fixation of the epiretinal implant.[59] In another study, it was reported that 9 of 10 rabbits were implanted without serious complications. The implant was stable at its original fixation area, and no change in retinal architecture underneath the implant was found by light microscopy. In 3 cases, mild cataract formation was observed, and in 1 case, a total retinal detachment was found after 6 months of follow-up.[75] In another study, 3 rabbits were implanted with an electrode array in the subretinal space. No side effects were reported.[63]

In a single case of implantation of optic nerve stimulating electrodes in a human, no acute or chronic side effects were noted.[52] No acute damage has been noted after electrical stimulation of the sciatic nerve of cats with similar cuff electrodes.[76]

2.1.2 *Attachment*. Any implanted electronic device will be exposed to movements and should be attached in a stable manner to its intended anatomical location. In particular, the epiretinal prosthesis will be exposed to countercurrent movements in response to ocular rotational movements that can reach a speed of 700 degrees visual angle per second.

The attachment methods differ according to different approaches and different locations along the visual pathways. The preferable fixation site of the intracortical microstimulation arrays is probably the cortex itself, and not the skull, because of the constant movement of the brain in relation to the skull. These arrays are currently inserted either by manual insertion of individual or groups of 2 to 3 electrodes normal to the cortical surface to a

Mark, Thesis 11/9/01 11:28 AM Page 276



depth of 2 mm[32] or by a pneumatic system that inserts 100-electrode arrays into the cortex in about 200 ms.[77]

The subretinal approach takes advantage of the adherence forces between the sensory retina and the retinal pigment epithelium to keep the array in place. On some occasions, though, the array can be displaced after implantation.[64] The surgical procedure is performed extraocularly through the sclera (ab-externo) or intraocularly through a retinotomy site after a vitrectomy procedure. One of the groups used a custom-made implantation tool to insert the device into the subretinal space.[48]

Bioadhesives, retinal tacks, and magnets have been some of the methods examined for epiretinal attachment. In 1 study, the retinal tacks and the electrode array remained firmly affixed to the retina for up to 1 year of follow-up with no significant clinical or histologic side effects.[59] Similar results were shown in rabbits.[75]

In another study, 9 commercially available compounds were examined for their suitability as intraocular adhesives in rabbits. One type of adhesive (SS-PEG hydrogel, Shearwater Polymers Inc) proved to be strongly adherent and nontoxic to the retina.[78] Others have conducted similar experiments.[79]

2.1.3 *Coating the electronics (hermetic seal).* All visual prostheses will consist of various electronic components. Implanted electronic elements such as data and power receivers and the stimulation processor must be hermetically sealed from the corrosive biological fluid.[10] This protective coating should last for several decades. The requirement of hermetically sealing a circuit in the case of neural stimulating devices is complicated by the demand that multiple conductors (feed-throughs) must penetrate the hermetic package so that the stimulation circuit can be electrically connected to each electrode site in the electrode array. These connections are the most vulnerable leakage points of the system.

The pacemaker industry has developed effective encapsulation using a hermetically sealed titanium case. Glass and ceramic packages have proved to be good hermetic cases as well. Integrated circuit electrodes and sensors require less bulky encapsulation. In the last few years, much attention has been focused on the development of miniature hermetic packages for microelectrode protection, though few provide a high number of reliable feedthroughs in a small volume.[80] Many types of welding or sealants tend to leak over time, are not biocompatible, and are expensive. The most encouraging results of hermetic packaging come from medical implant companies, such as Advanced Bionics (Sylmar, Calif), that involve novel use of organic polymers in combination with either ceramic or titanium cases.[81]

Yet another hermetic packaging technique is based on electrostatic (anodic) bonding of glass to silicon. The process generates a high electric field at the glass-silicon interface and causes a permanent and irreversible fusion bond between silicon and glass.[10,82,83] Using a silicon substrate allows many micron scale feed-throughs to be micromachined into the hermetic package. Recently, a new technique of aluminum/silicon-to-glass solder bonding was developed. This technique provides more than 10 megapascals of bonding strength and a good hermeticity.[84]

In summary, techniques for coating the electronics are a fundamental step to the future feasibility of any visual prosthesis, which has the daunting hurdle of hermetically sealing a small electronic package with a high number of feed-throughs.

*2.2 Electrical Stimulation Biocompatibility*

2.2.1 *How much current can be used before impairing the physiological function of the cells?* When applying electrical stimulation, neural damage limits need to be considered. Among the early studies that have had a significant impact on this field are the histopathologic studies of long-term stimulation of neural tissue[85-87] and the electrochemical studies of the electrode-electrolyte interface.[88] The relative safety of biphasic charge balanced waveforms compared to monophasic waveforms was demonstrated.[89]

Any net direct current (DC) can lead over time to irreversible electrolyte reactions. A biphasic current waveform consisting of 2 consecutive pulses of equal charge but opposite polarity has no DC component. A simple monophasic waveform is unacceptable for neural stimulation because it delivers DC and creates irreversible faradic processes. Faradic reactions involve electron transfer across electrode-tissue interface and oxidation/reduction of chemicals. It is also necessary to know the chemical reversibility of electrode materials and stimulation protocols. Chemical reversibility requires that all processes occurring at an electrode subjected to an electrical pulse, including $H_2$ and $O_2$ evolution, will be chemically reversed by a pulse of opposite polarity. Chemical reversibility can be examined by cyclic voltammetric analysis[90] and other methods such as direct observation of gas bubbles, UV spectroscopy, or atomic absorption spectrometry of in vitro pulse solutions. Corrosion effects on electrode surfaces can be examined by scanning electron microscopy.

It was shown that electrical stimulation–induced neural injury is dependent on current amplitude and pulse frequency, but more important, on charge density and charge per phase.[91-93] The charge per phase is defined as the integral of the stimulus current over half (1 phase) of 1 cycle of the PD. Charge density is defined as charge per phase divided by the electrochemically active surface area of the electrodes. From these definitions, it can be understood that very small electrodes can produce very low

Mark, Thesis 11/9/01 11:28 AM Page 277



current thresholds, yet may produce unacceptably high charge densities. Since total charge density is responsible for the damage of tissue and electrodes, there is a theoretical limit as to how small the electrodes can be.[94,95] Total charge delivered to the tissue cannot be ignored, even though it is within safe limits of the size of the electrodes being used. Put another way, the threshold for neural damage is related not only to the charge density, but also to the total charge.[92,96]

Using simple waveforms, conservative charge density/charge limits for chronic stimulation with platinum are 100 $\mu C/cm^2$ and 1 $\mu C$/phase. For activated iridium oxide (IrOx) electrodes, the limit is 1 $mC/cm^2$ and 16 nC/phase. Nevertheless, chronic stimulation can reduce the maximum charge density that is safely injectable.[97] Many of the studies that were done to determine these limits were performed in cortical tissue[91,92] or obtained from studies on electrical stimulation of the auditory nerve.[98]

In spite of all the limitations and difficulties, it was found that neural stimulation with electrical pulses can be safe and have stable, effective long-term results.[93,99,100] It was also shown that transient changes in neural response properties, such as stimulation-induced depression of neuronal excitability, are caused by electrical stimulation, but these have not been correlated to histologically detectable tissue damage.[93,96,101] In other studies, it was shown that repeated stimulation did not change the threshold amplitudes over time since implantation.[19,28,52]

Despite established safe limits for neural stimulation, long-term in vivo retinal stimulation must be performed before any conclusions regarding threshold stimulation parameters of the retina are made. The reason is that the threshold at which damage occurs cannot be freely extrapolated from 1 neural tissue to another.[102]

2.2.2 *How much heat can the device produce?* Different components of the visual prostheses can produce excessive heat and cause damage if not kept below a certain limit. Many of the studies regarding thermal exposure damage studied the effects of microwave and other electromagnetic field exposures. The safe limit is usually considered to be 1.6 (0.06ºC) or 8 W/kg (0.3ºC) (uncontrolled or controlled exposure to microwave radiation, respectively), above which any heating would be undesirable.[103] The retina's ability to dissipate and tolerate heat generated by an intraocular electronic heater was studied in 16 dogs. It was shown that no more than 50 mW of power over a 1.4 $mm^2$ area can be applied directly onto the retina for more then 1 second. However, using the same heater, a power of 500 mW in the midvitreous for 2 hours did not cause any histologic damage. It was concluded that heat-producing components of the device (coils for radio frequency telemetry and electronic chips) should be placed far away from the retina, probably right behind the iris and/or in the midvitreous. Placing the electronics directly in contact with the retina, either epiretinally or subretinally, has a high risk of causing heat injury. Thus, only the electrode array, which produces a relatively small amount of heat, should be put in direct contact with the retina.

2.2.3 *Powering the implant*. Supplying adequate electrical power is a concern for any implantable electronic device. Some electrical stimulators for chronic pain treatment use a battery and rely on repeated surgery to replace it. Alternatively, it is possible to power implants without a physical connection (wirelessly) through an inductive link. Inductive links are commonly created between 2 coils of metallic wire, with a primary coil (the coil that has a signal directly applied by a circuit) and a secondary coil (the coil in which a current is induced).[104] Pacemakers and cochlear implants are inductively powered. There are several parameters that can be adjusted when designing an inductive link. These parameters include the diameter and turns of the primary and secondary coils and the relative position of the 2 coils. Large primary and secondary coils may be undesirable for aesthetic reasons and anatomical constraints, respectively. Power transfer is maximized if the coils are coplanar.[105] This is not practical for most implants, and the coil planes are slightly offset, decreasing efficiency for what is already an inefficient method of transferring power. Typical power transfer rates are approximately 2%. The primary reason for this inefficiency is the fact that the magnetic field spreads indiscriminately from the transmitter. Nevertheless, the average power supply to drive both the inductive link and the stimulator chip (for 100 electrodes) is around 5 mW.[106] Mathematical estimates of millimeter-sized coils have estimated that up to 50 mW of power can be recovered using a 9 cm-diameter primary coil and a 1.5 mm secondary coil.[106] These calculations show that enough energy can be delivered into the eye by this method. Alternatives have been proposed for delivering power to ocular implants, taking advantage of the transparent optical pathway. One conceptual device included a laser that would excite implanted photodiodes to produce electric current. While this link would be more efficient than the inductive link, since the laser could be targeted, it raises safety concerns owing to the known deleterious effects of laser light on the retina.[60]

One subretinal device that does not have any external connections is powered solely by incident light with wavelengths of 500 to 1,100nm.[64] This same principal is used by another group.[48,107] One of the disadvantages of this method is the amount of light that must reach the array. The light intensity needed to activate the photosensors is in the range of 600 to 1,800 $W/m^2$.[108] This range is far beyond the sunlight intensity on earth (fluorescent light 10 $W/m^2$, sunlight

Mark, Thesis 11/9/01 11:28 AM Page 278



100 W/m$^2$). To overcome this problem, additional energy in the near infrared light was added to the spectrum of solar cells of the microphotodiode.[109] The infrared light is tolerated by the retina up to intensities of 200 mW/cm$^2$, in contrary to the visible light (100 mW/cm$^2$). However, additional microelectronic circuitry to process and direct this power is necessary, and the concomitant heat dissipated by such a device may lead to retinal damage.

2.2.4 *Electrodes*. The electrode array is in direct contact with biologic tissue. Thus, it has the potential to damage the tissue mechanically, chemically, and physically, and vice versa,[110] The electrodes' charge transfer efficiency will affect every subsystem of the prosthesis by influencing the power requirements and the electrode density.

Different materials were tested for the fabrication of electrode arrays. Even the "noble" metals (platinum, iridium, rhodium, gold, and palladium) corrode under conditions of electrical stimulation.[111,112] Platinum and platinum-iridium alloys are the most widely used for neural stimulating electrodes because of its resistance to corrosion and considerable charge-carrying capacity. The unavoidable dissolution of platinum under electrical stimulation decreases when a protein is included in the solution and with continuous stimulation.[112]

Iridium oxide electrodes belong to a new category termed "valence change oxides." IrOx has been used in research for nearly 20 years, but a commercial microstimulator with a single IrOx electrode (BION, Advanced Bionics) has only recently been approved for human use. IrOx is exceptionally resistant to corrosion. The charge density limit for chronic stimulation is 1 mC/cm$^2$, and it has a safe stimulation limit of 3 mC/cm$^2$ in vitro.[113] IrOx electrodes have been proved to withstand more than 2 billion 10-mA current pulses without degradation.[10]

Recently, a titanium nitride (TiN) thin-film electrode has demonstrated charge injection limits of 23 mC/cm$^2$, higher than both platinum and IrOx.[114] Though TiN electrodes have better mechanical properties than IrOx electrodes, they seemed to have adverse effects on retinal cells' survival when in direct contact. However, it was clear that no soluble factor is responsible for decreased cell survival, and they are still used for fabricating electrode arrays.[48]

When trying to figure out the accepted dimensions of electrodes, one should refer to safe charge density measurements. For example, as was discussed earlier, the charge injection limits for platinum and IrOx electrodes are 100 μC/cm$^2$ and 1mmC/cm$^2$ respectively. Thus, the maximum sizes based on a 1-μC charge requirement for threshold intraocular stimulation of patients with RP would be 0.01 cm$^2$ and 0.001 cm$^2$ for platinum and IrOx, respectively. For disc electrodes, these values correspond to minimum disc radii of 0.56 mm for platinum and 0.18 mm for IrOx. In addition, experiments with frog retinas demonstrated that a 3-dB rise in threshold occurs in about 0.25 mm. So, edge-to-edge separation between neighboring disc electrodes should be no less than 0.25 mm.[115]

Another possibility is to use capacitor electrodes. These electrodes operate without any faradic reactions. A thin surface layer of dielectric material insulates the metal from the solution and prevents electrochemical reactions. The most practical material is anodized tantalum because of the small amount of DC leakage. However, these electrodes have lower safe injectable charge density and charge storage ability when compared to platinum, IrOx, and TiN electrodes.[116]

The charge density limits are measured for uniform current distribution. However, because of certain geometric considerations, neural prosthetic electrodes are likely to have nonuniform current distributions, which can exceed the chemically reversible limits.[117] For example, it has been shown that disc electrodes create uneven current density, with the highest densities or "hot spots" being near the edges of the disk. If the disks are recessed even to a small depth, the current density is more evenly distributed.[118]

Some of the methods used for the visual prosthesis deserve special considerations. The subretinal device is composed of subunits measuring 20 x 20 μm. Every subunit is a combination of a silicon microphotodiode and a stimulating electrode. The density of the subunits is 1,100 subunits/mm$^2$. This device can theoretically create a barrier between the retina and the choroid, which provides nourishment to the outer layers of the retina. To prevent the barrier effect, 1 of the groups incorporated porous electrode array structures to facilitate nutritional exchange between the retina and the underlying choroid. The size requirements will limit the power of the subretinal implant.[64] In addition, the electronic device creates heat, which may affect the delicate sensory retina above it. Patches of fibrosis and RPE changes were observed after chronic subretinal implantation, and histologic examination of the retina showed declining inner nuclear and ganglion cell layer densities[64] but no inflammatory response. Another report showed that there was irregular glial proliferation above the electrode array.[48]

The principal difference between the cortical and retinal prostheses is the design of the electrode array. As was discussed earlier, the cortical electrode array should probably consist of penetrating microelectrodes. One group, developing a cortical implant, has focused on the use of doped silicone for their penetrating electrode array for cortical stimulation.[33] The tips of the 1.5/1.0 mm long electrodes are covered with platinum. The array typically looks like a nail bed and consists of 100 penetrating electrodes. The diameter of each electrode at its base is 80 to 100 μm and 2 to 3 μm at the tip. Chronic implantation of this electrode array varied from no reaction at all to a

Mark, Thesis 11/9/01 11:28 AM Page 279



thin capsule around each electrode track, to extensive gliosis with buildup of fibrotic tissue between the array and the meninges, resulting in array displacement and bleeding.[33] Thin capsules around electrode tracks and tissue accumulation on pulsed CNS electrodes were also reported by others.[93-97] Nevertheless, tissue encapsulation does not always preclude effective stimulation.[97,119]

Another electrode technology uses silicon micromachining to fabricate multichannel arrays for neural prostheses applications. Microfabricated silicon electrodes were initially conceived in the early 1970s.[120] In the subsequent years, the dimensions of these electrodes have been decreased, utilizing the concurrent advances in the microelectronics industry. Today, micromachined silicon electrodes with conducting lines of 2 μm are standard.[121-124] These fabrication processes have been advanced by the microelectronics industry and therefore allow the integration of microelectronics and the electrode array into a monolithic device. The primary reason for the inclusion of on-chip electronics in such a device is to minimize the number of external leads required between the electrode sites and the outside world. Recording/stimulating sites are located along the silicone probe substrate. These probes are capable of extracellular recording/stimulating of many cells in neural tissue simultaneously on a spatially distributed basis.[82,125-129] Chronic implantation and in vitro testing have demonstrated the ability of silicon devices to maintain electrical characteristics during long-term implantation.[97]

Some general conclusions can be drawn from the preceding discussion. A stimulating electrode array must meet several requirements. These include a high number of densely packed electrodes to provide a high acuity image and individual electrodes that can safely inject a large amount of charge. Current electrode technology that is employed in neural prostheses uses handmade electrode arrays with a small electrode count (up to 32), most likely an insufficient number for a visual prosthesis. Micromachining technology has been used to fabricate electrodes for neural stimulation, but these devices have not been optimized for use in the eye.

The global shape of the array, the shape of each electrode, the way to insert and attach it, and other factors depend on the anatomical location of stimulation. If either IrOx or TiN electrodes can be successfully incorporated into a visual stimulating array, then the potential advantages include more input channels, higher image quality, and reduced power consumption.

### 3. SCOPE OF THIS THESIS

Because of the enormous number of scientific disciplines involved in constructing and showing the feasibility of an electronic retinal implant, it is easy to lose focus and get overwhelmed. However, the 2 most critical pieces of the development effort that remain not completely solved are that of optimizing electrical stimulation parameters for the retina and defining the number of electrical contacts needed with the retina to enable useful vision. Delineating these parameters is at the crux of the engineering of the electronic implant, as it has direct consequences on power requirements, heat dissipation, image processing, and the safety of the retinal and other ocular tissue. In this thesis, we address these issues through different experiments. The first set of experiments uses 2 different electrophysiological setups to optimize the stimulating parameters. The second set of experiments uses psychophysics to determine the number of inputs and image processing that would be needed to provide useful vision.

## METHODS

### 1. ELECTROPHSIOLOGIC EXPERIMENT

All animal protocols used in this study were in accord with the Association for Research in Vision and Ophthalmology guidelines for animal care and use as well as approved by the Johns Hopkins Animal Care and Use Committee.

*1.1 In Vivo Mouse Experimental Setup*

1.1.1 *Animal model and preparation of the retina.* Three different groups of mice were used in this study: 8-week-old normal-sighted male mice C57BJ/6J (Jackson Labs, Bar Harbor, Me), 8-week-old retinal degenerate (rd) male mice C3H (Charles River, Wilmington, Mass), and 16-week-old rd male mice. The mice were anesthetized with an intraperitoneal injection of ketamine (80 mg/kg, Ketaject, Phoenix Pharmaceutical, St Joseph, Mo) and xylazine (10 mg/kg, Xyla-ject, Phoenix Pharmaceutical). The mouse was given subsequent doses every half hour to maintain it at the initial plane of anesthesia. The body temperature of the mouse was maintained at 35°C with a heating pad (Frederick Haer, Inc, Bowdoinham, Me). At the conclusion of the experiment, the mouse was sacrificed by a lethal dose of pentobarbital injected intraperitoneally (120 mg/kg).

For the surgical procedure, the mouse was placed in a custom-built stereotactic head holder to maintain the head in a fixed position and to allow access to the eye. The holder was placed under a light microscope on a vibration-isolated table. A 30-gauge needle was used to make a small incision in the cornea. Next, the central corneal button was removed using scissors. Sodium hyaluronate (Healon GV, Pharmacia, Columbus, Ohio) was injected behind the lens to deliver the intact lens out of the eye and to prevent the eye from collapsing. Finally,

Mark, Thesis 11/9/01 11:28 AM Page 280



the recording and stimulating electrodes were positioned on the retinal surface optic (Fig 4).

1.1.2 *Retinal recording.* Two tungsten-recording microelectrodes (5 Mohm, A-M Systems, Everett, Wash) were positioned on the retinal surface with a micromanipulator (MX-100, Newport, Irvine, Calif). A ground electrode was placed in the mouth. A differential amplifier (Dagan Corporation, Minneapolis, Minn) was used to condition the signal (20 K gain, 0.3 to 3 kHz). Data acquisition and stimulus output were accomplished via a commercial electrophysiology system (ACDaq, Seattle, Wash).

1.1.3 Light stimulation. Light responses were obtained by full-field illumination from a 1,000-lumen Xenon light source (model 201, ILC Technology, Sunnyvale, Calif) coupled to a fiber optic light probe. Light was delivered to the surface of the retina via the fiber optic light pipe. Retinal recordings were synchronized to the light stimulus through the use of a computer-controlled light shutter (Uniblitz T132, Vincent Associates, Rochester, NY).

1.1.4 *Electrical stimulation.* A 125 μm-diameter platinum wire was used to stimulate in a monopolar configuration (ie, the current return electrode was placed at a distance on the tail of the animal). The stimulus output waveform was converted to constant current by a stimulus isolator. Electrical stimulation was performed in dark conditions. Several stimulus waveforms were used. The first half-pulse was cathodic and the second half-pulse was anodic. There was no delay between the cathodic and anodic phases. All trials were performed using charge-balanced waveforms. Response threshold as a function of stimulus strength was determined for several waveforms. A single biphasic pulse was investigated at 5 pulse durations (40, 80, 120, 500, and 1,000 μs). A single cycle of a 1-kHz sine wave was also used. Finally, pulse trains were investigated (5 x 40 μs, 10 x 40 μs, 5 x 80 μs, 10 x 80 μs, 5 x 120 μs, and 10 x 120 μs) to compare with single pulse. Stimulus threshold was defined as the stimulus that would elicit an action potential in 2 of 3 trials. Action potential threshold was set to 3x peak noise (noise was typically ±10 μV).

The threshold charge was statistically analyzed using a Student *t* test for comparison of 2 sets of data and ANOVA for comparison of multiple data sets. A $P < .05$ was considered statistically significant.

*1.2 In Vitro Retinal Isolate Experiments*

1.2.1 *Retinal harvesting and maintenance.* Thirty-eight adult (~ 2 kg) Dutch belted rabbit eyes were anesthetized with 2 cc of a mixture of 60% ketamine (80 mg/kg, Ketaject, Phoenix Pharmaceutical) and 40% xylazine (10 mg/kg, Xyla-ject) through intramuscular injection. The eye was

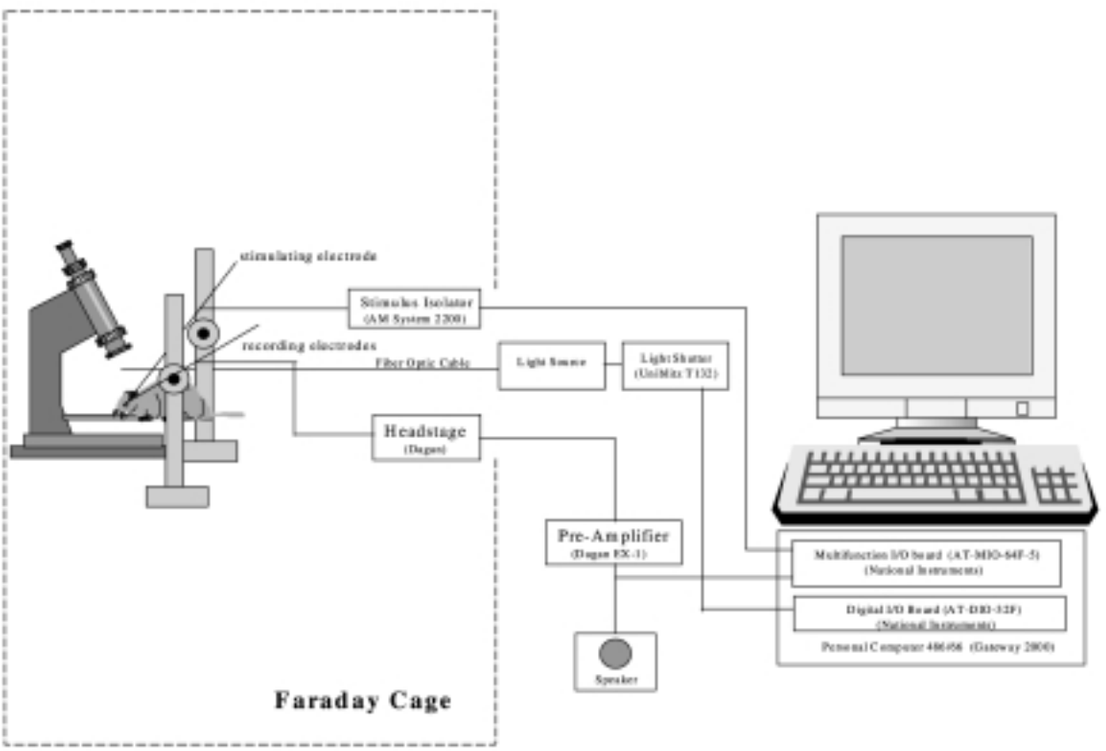


**FIGURE 4**

Setup for in vivo mice retinal recordings, which is inside a Faraday cage. Under computer control, either a light or an electrical stimulus can be delivered and a retinal ganglion cell response simultaneously recorded.

Mark, Thesis 11/9/01 11:29 AM Page 281



enucleated, and the retina was dissected out of the eyeball, and then transferred to Ames' medium (Sigma Chemical Co) bubbled with 95% oxygen and 5% carbon oxide and heated to 37°C. A heated chamber (ORC-1, Center for Network Neuroscience, University of North Texas, Denton) was used to hold the retina and allow a flow of solution through the chamber (Figs 5 and 6)

1.2.2 *Stimulus and recording electrodes*. Two types of stimulation electrodes were used: platinum macroelectrode (125 μm and 25 μm diameter, Frederick Haer, Inc) and a photolithographically defined microelectrode array (MMEP4, Center for Network Neuroscience). The MMEP4 has an 8 x 8 grid of 22 μm-diameter gold electrodes patterned on a glass plate. Two identical electrodes were used in dipole configuration, 1 as the current source and the other as the current sink. MMEP electrodes were at a fixed distance of 100 μm. The macroelectrodes were positioned individually, but the edge-to-edge distance was estimated to be 300 to 400 μm based on the known diameter of the outer cannula. Electrical stimulation was performed with the stimulating electrodes on either the ganglion cell surface or the photoreceptor surface. Two penetrating tungsten electrodes (A-M Systems) were used for differential recording and set between optic disc and the stimulation electrodes. The retinal location of the recording electrodes was verified by recording spontaneous and light-driven action potentials. The distance between stimulation and recording electrodes was approxiamtely 2 mm. Six test conditions were studied: 3 electrodes (MMEP, 125 mm, and 25 mm) each in 2 positions (PR-stimulating electrodes on photoreceptor surface and GL-stimulating electrode on ganglion cell surface).


**FIGURE 5**
Isolated retinal setup, which is housed inside a Faraday cage. Metallic ring overlies an electrode array, forming a watertight chamber for retinal tissue. Chamber is connected to oxygenated, heated Ames media via rubber hoses.

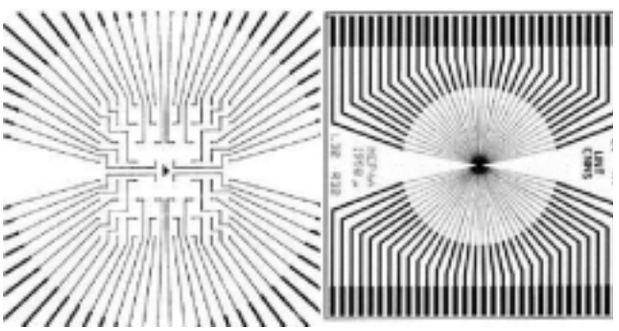

**FIGURE 6**
Photomicrograph of Indium-tin-oxide electrode array (MMEP array). Wires terminate in small electrodes that are used to stimulate overlying retinal tissue.

1.2.3 *Stimulus and recording parameters*. Stimulus generation and data acquisition were controlled by a computer-based system (ACDaq, AC Instrumentation, Seattle, Wash). A battery-powered preamplifier (P15, Grass Instruments, Quincy, Mass) was used for initial filtering and amplification (10x gain, and a bandwidth of 3 to 300 Hz). A second filter (Dagan Corporation) was used to condition the signal. The combination of the 2 filters yielded a 20-K gain and a bandwidth of 0.3 to 3 kHz. Light responses were obtained in response to a light stimulus from a 1,000-lumen Xenon light source (model 201, ILC Technology) coupled to a fiber optic light probe. Retinal recordings were synchronized to the light stimulus through the use of a computer-controlled light shutter (Uniblitz T132, Vincent Associates). Current pulses were generated by a custom-built voltage-to-current converter under computer control.

1.2.4 *Stimulus waveforms*. In each of the 6 electrode configurations, biphasic stimulus pulses were applied. All pulses were cathodic first with a 4-ms delay between the first and second phase. The pulses were varied in phase duration (0.1 ms, 0.5 ms, and 1 ms). The initial stimulus amplitude was set to 3.2 μA and increased in steps of 1.6 μA until a response was elicited. The threshold of the response was defined with the response rate over 3 quarters. We also double-checked the responses with other waveforms. The latency was defined as the time from the end of the stimulus to the beginning of the response at the threshold stimulus. For statistical analysis, the natural logarithm of each value was used to do ANOVA and *t* tests.

## 2. PSYCHOPHYSICAL TESTING

### *2.1 Facial Recognition*

Subjects were 4 college graduates aged 25 to 32 years of age. The subjects were volunteers with a best corrected visual acuity of 20/20. Prior to their participation in the study, written informed consent was obtained from all participants and each participant was given a copy of the signed consent form.

The facial images for the study were composed of a database of 60 patients and hospital employees. The group was composed of equal numbers of men and

Mark, Thesis 11/9/01 11:29 AM Page 282



women and black and white individuals. In each of these 4 groups were equal numbers of "old," "middle aged," and "young" individuals. Using a digital camera with a resolution of 640 x 480 pixels with 256 gray levels, 1 straight-on image and 4 averted images of each individual were captured for use in the study. Facial images displayed occupied a visual field of 13° horizontally when measured from ear to ear.

With use of Microsoft Visual Basic, software was developed to perform the facial recognition task using a 400-mHz Pentium II personal computer, a Diamond Stealth video card with 2 megabytes of memory, with video output to a modified Low Vision Enhancement System (LVES) display. The LVES display has a vertical visual field of 36° and a horizontal visual field of 48°. The display has 480 vertical pixels and 640 horizontal pixels. Thus, each pixel represents 4.5 minutes of arc. The LVES is capable of displaying 256 gray levels.

The LVES head-mounted display was fitted to each subject. A test screen was then utilized for subjects to focus the image to correct for refractive errors in their right eye. In the monocular trials, subjects viewed a test set of 4 facial images displayed using the full resolution of the display. The 4 faces in each trial were matched for sex and race (Fig 7).

After these images were reviewed, subjects depressed the space bar to view the test image, start the viewing timer, and clear the screen. The test image was an averted facial image of 1 of the individuals seen in the test set. Subjects viewed the test image by scanning a grid of dots, simulating pixelized prosthetic vision over the averted facial image using a mouse-pointing device (Fig 8).

Upon determining the identity of the test image, subjects again depressed the space bar. This stopped the viewing timer and returned the display to the original test set of 4 facial images. Using the mouse-pointing device, subjects matched the face in the test image with 1 of the 4 faces from the test set. Subjects performed 204 trials with the test images viewed under high-contrast conditions with a background level of 0. During the trials, the dot size, dot spacing, grid size, number or gray levels, and dropout percentage were varied. A second trial was then conducted in which the test images were viewed under low-contrast conditions with a background gray level set at 30% for all 3 primary colors (red, green, and blue).

### *2.1 Letter/Symbol Recognition and Activities of Daily Living*

Hospital employees and undergraduate students were recruited as volunteers. All 8 volunteers had 20/30 vision or better either without correction or with contact lens correction.

A PC video camera captured images that were converted into pixels by real-time software. The pixelized image was displayed on the PC monitor as well as on a head-mounted display (HMD) worn by test subjects. The camera used was Logitech QuickCam Pro, which has the following specifications: manual focus lens type 6 mm, f=2.0, field of view 46° and a CCD resolution of 640 x 480 pixels (VGA specification). The pixelizing software filter was provided by Second Sight, LLC, Valencia, Calif. It converts the entire video image into an array of discrete squares ("pixels"). Each pixel is a solid gray-scale figure representing a mean luminance across its aperture in the image captured by the camera. For example, if the target area for 1 pixel were centered on a black object larger than the pixel's aperture, the pixel would be black. However, if the camera was redirected so that the pixel's target area was half on the black object and half on a white

**FIGURE 7**
Representative set of four faces used in face discrimination protocol.

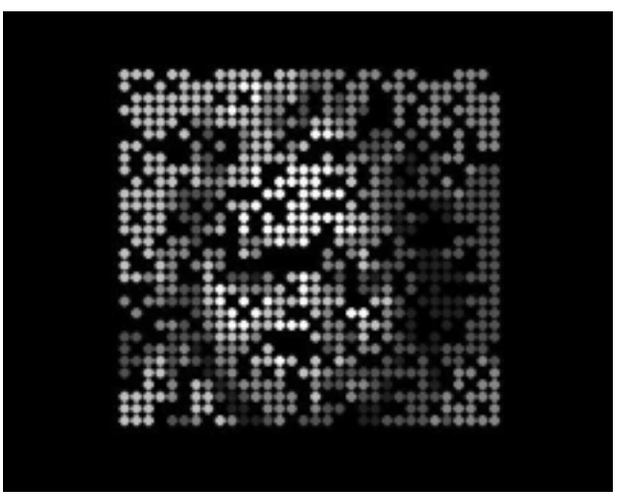

**FIGURE 8**
Appearance of a face after it has been pixelized using the modified Low Vision Enhancement System (LVES).

Mark, Thesis 11/9/01 11:29 AM Page 283



background, the entire pixel would be medium gray. Adjustable property settings of the filter include number of rows, columns, gray scale levels and the height and width of percentages of each pixel (with the remaining portion being a gray gap between adjacent pixels). To provide a realistic rendition of dynamic range and resolution expected from a retinal prosthesis, maximum contrast (100%) and number of simultaneous, gray-scale levels (6) were held constant. All other properties were adjusted for the individual arrays (see below). A Belkin Expand View video output splitter enabled us to display identical images on the HMD by test subjects and our PC monitor for observer viewing. The HMD, a PLM-100 Personal Video Headset by Sony, resembles a large visor and contains 2 0.7-inch LCDs projecting 1 to each eye. This monitor has a "see-through" feature, which normally allows the wearer to see the real world while simultaneously viewing a transparent image of the monitor. To eliminate outside visual input, subjects wore a black felt blindfold over the HMD. Making no other adjustments, we utilized all standard display parameters.

According to the parameters described above, the actual 4 x 4 array will cover 7.3° of retina in both the x axis and the y axis. (1.3° for each of the 4 electrodes and 0.7° for each of the 3 spaces). The 16 electrode pixelized simulation was sized such that the angle subtended by the image composed 7.3° of the subjects' visual field. We assumed the same electrode diameter and spacing for the 6 x 10 electrode array as the 4 x 4. This translates to 11.3° in the y axis and 19.3° in the x axis. The physical sizing of the simulated array was done as described for the 4 x 4 array. The dimensions of our 16 x 16 electrode array were restricted to fit within a 3.5 mm scleral incision. The y axis of the 6 x 10 array would do just that, so we use the same arc length here in both axes (11.3°). This simulation assumes the eventual capacity to manufacture small electrodes with safe charge densities. Again, a template was made for sizing of this electrode as in the previous 2. Last, the size of the entire array established, the height and width percentage of the pixels were altered such that spaces between pixels were approximately one-half the size each pixel.

2.1.1. *First set of tasks*. The first set of tasks involved obtaining visual data at a distance ranging from 10 to 70 cm. The camera was placed in a modified adjustable head strap in a midline position above the eyes. This allowed subjects to control the camera with head movements. All 4 tasks in this first set were completed with the 4 x 4 array then repeated with the 6 x 10 array and finally with the 16 x 16. The expected visual acuities are 20/2400 for the 4 x 4 and 6 x 10 arrays and 20/865 for the 16 x 16 array.

2.1.1.1 *Tumbling E*. With the test subject seated, a standard 20/200 E (8.8 cm tall; size of each branch was 20% of the height) was placed in front of them on a large white background. They were asked to identify which direction the E was facing (ie, up, down, left, or right). They began at a distance of 70 cm. If they could not identify the direction, the distance was decreased to 50 cm, then 30 cm, and finally 10 cm. The distance at which they first recognized the orientation of the E was recorded for each array. It was assumed that subjects could correctly identify the orientation at closer intervals once they have done so for a given distance.

2.1.1.2 *Object recognition*. A plate, cup, spoon, and pen were placed on a black table sequentially in front of the subject for a maximum of 3 minutes each. The only information about the objects given was that they were all common items that most people use on a daily basis. Subjects were instructed to describe the object's shape, size, and overall appearance. If they thought they could identify the object, they were asked to say "My guess is…." They were allowed only 1 guess per object. An accurate description but incorrect guess was awarded 1 point. A correct guess was awarded 2 points. No points were given for inaccurate descriptions.

2.1.1.3 *Candy pour*. Two white cups were placed 5 to 10 cm apart on a black table. The cup in front of the subject's dominant hand contained 10 pieces of hard candy, and the other cup was empty. The subject's task was to pick up the full cup with the dominant hand and pour the candies into the empty cup touching it neither with the hand nor with the full cup. The number of candies successfully poured into the empty cup was counted.

2.1.1.4 *Cutting*. A hollow black rectangle printed on a standard sheet of white 8.5 x 11-inch paper was handed to the subject. The task was to cut around the outside of the black rectangle on all 4 sides. Total cutting time was noted. Accuracy was judged by measuring the distance between the cut and the actual target. If the cut was 1 cm or less from the target, this was judged to be correct. The cumulative length of the correct cut was measured and recorded as a percentage of the length of all 4 sides of the rectangle (59.2 cm).

2.1.2 *Second set of tasks*. The second set of tasks required that the camera be quite steady and very close to the object. To accomplish this, the video camera was mounted on a platform such that the lens was 4.5 cm from the target. There were also 2 straight edges on the table that helped maintain the camera and the viewing material in the proper orientation for reading during scanning.

2.1.2.1 *Symbol recognition*. With the 4 x 4 array, subjects scanned over 3 symbols on a Light House Key Card. Correct responses ("house," "circle," "square") were awarded 2 points, close responses were awarded 1 point, and inaccurate responses were awarded no points.

2.1.2.2 *Reading*. The Minnesota (MN) Read Acuity

Mark, Thesis 11/9/01 11:29 AM Page 284



Chart (A) was used for reading material. This chart consists of sentences of 10 to 12 words. Each is printed in a progressively smaller Courier bold font. With the 6 x 10 array, subjects were asked to read the first sentence (72-point font). With the 16 x 16 array, they were asked to read the first 5 sentences. Time required to complete each sentence, as well as the number of words read correctly, was recorded.

## RESULTS

### 1. ELECTROPHYSIOLOGIC RESULTS

*1.1 In Vivo Mice Experiments*

A light-driven response was easily obtained from normal mouse but could not be obtained from either 8-week-old or 16-week-old RD mouse, despite multiple placements of the recording electrodes (Figs 9 and 10).

Single-unit spontaneous activity was obtained from all 3 mouse groups. The spontaneous activity was used to determine when the recording electrode was in the proximity of the ganglion cells. Electrical elicited responses were obtained from each group: 8-week-old normal mouse (n=14), 8-week-old rd mouse (n=15), and 16-week-old rd mouse (n=10). The charge threshold was compared across all 3 groups and for different waveforms within the same group.

In normal mouse, a single cycle of a 1-kHz sine wave was significantly more efficient than a 1-kHz square wave ($P$ <.05) (Fig 11), but no such difference was noted in either of the rd mouse groups (8-week-old, $P$ = .426; 16-week-old, $P$ = .0783) (Fig 12).

Charge threshold was significantly higher in 16-week-old rd mouse versus both 8-week-old rd and normal mouse for every stimulus duration ($P$ <.05). In all groups, short-duration pulses (40, 80, and 120 μs) were more efficient in terms of total charge (the product of pulse amplitude and pulse duration) than longer (500 and 1,000 μs) pulses ($P$ <.05). However, much more total current was required to elicit a response with short pulses. In all groups, applying a pulse train did not lead to more efficient charge usage ($P$ <.05).

*1.2 In Vitro Retinal Isolate Experiments*

For photoreceptor-side stimulation, macroelectrode stimulus threshold current was significantly lower than threshold current delivered with the MMEP ($P$ <.05) (Fig 13). When using the MMEP for stimulation, ganglion cell surface stimulus threshold was significantly lower than photoreceptor-side stimulus threshold ($P$ <.05). No difference between ganglion cell stimulation and photoreceptor-side stimulation existed using the macroelectrodes. For all groups, the stimulus current thresholds of 1-ms pulse-width groups were significantly lower than those of 0.1-ms

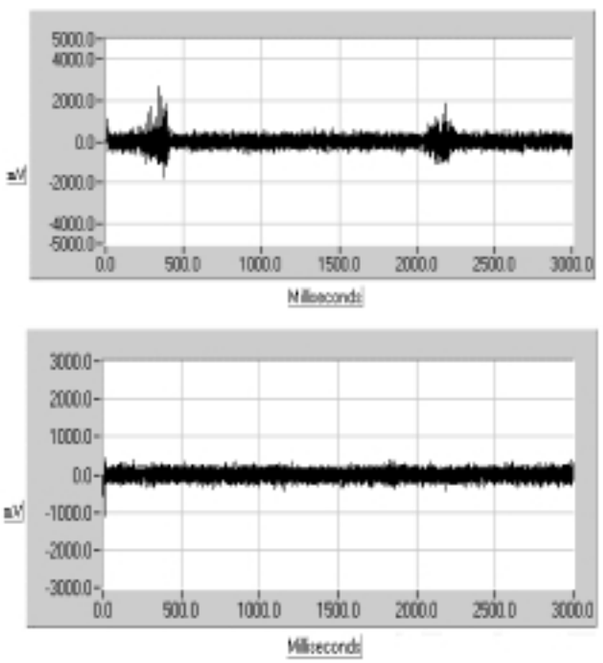


**FIGURE 9**

Top, Light-driven retinal ganglion cell response from normal mouse. Two distinct bursting neuronal activities were recorded at onset and offset of light stimulus (ie, On and Off responses, respectively). Bottom, Absence of such light-driven retinal ganglion cell responses in rd mouse.

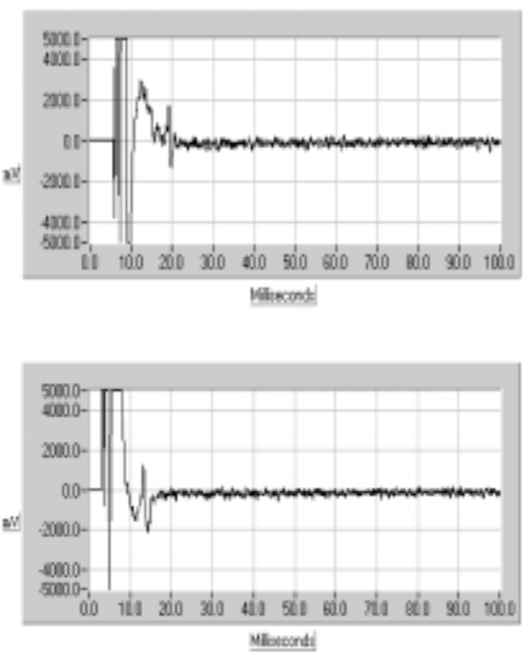


**FIGURE 10**

Electrically elicited retinal ganglion cell (RGC) response. First tracing above baseline is stimulus artifact. RGC response can be seen at 20 and 15 ms in top (normal mouse) and bottom (rd mouse) pictures, respectively.

Mark, Thesis 11/9/01 11:29 AM Page 285



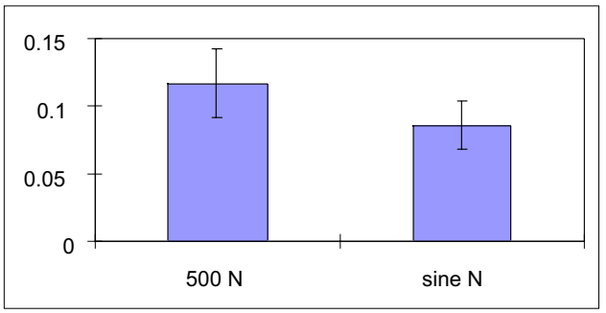


**FIGURE 11**

Thresholds charge to elicit a retinal ganglion cell response in normal mouse with either a 500-micropulse-wide square wave (500 N) or a 1-kHz sine wave (sine N). The y axis units are microcoulombs. Bars denote standard deviations.

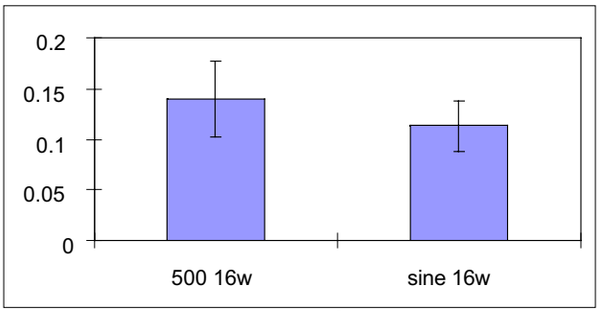


**FIGURE 12**

Thresholds charge to elicit a retinal ganglion cell response in a 16-week-old rd mouse with either a 500-micropulse-wide square wave (500 N) or a 1-kHz sine wave (sine N). The y axis units are microcoulombs. Bars denote standard deviations.

pulse-width groups. Response latency was studied with 1 ms pulses for both electrodes and stimulus sites (Fig 14). All groups demonstrated similar latency except the MMEP/PR group.

## 2. PSYCHOPHYSICAL TEST RESULTS

### *2.1 Face Recognition*

In high-contrast tests, facial recognition rates of over 75% were achieved for all subjects with dot sizes of up to 31.5 minutes of arc when using a 25 x 25 grid with 4.5 arc minute gaps, a 30% dropout rate, and 6 gray levels (Fig 15).

This corresponds to sampling with at least 11 cycles per face horizontally, ear to ear. The results deteriorated when sampling lower rates, 7 cycles per face or less (Fig 16).

All subjects were able to correctly identify at least 75% of the facial images with dot gaps of up to 31.5 minutes of arc when using a 25 x 25 grid with 13.5 minute dots a 30% dropout rate, and 6 gray levels (Fig 17).

In testing increases in gap size, facial recognition rates dropped when the sampling interval dropped from 9 cycles per face to 7 cycles per face. Using a 25 x 25 grid spanning a field of 7.5° or a 32 x 32 grid with a field of 10º, subjects achieved facial identification rates over 80%. All subjects achieved facial recognition rates of over 80% in resolution testing with 6 gray levels and dropout rates of less than 30% (Fig 18).

High-contrast facial recognition rates exceeded low-contrast facial recognition rates. During low-contrast testing, facial recognition rate of over 80% for all subjects was achieved only with a 25 x 25 grid, with 13.5 arc minute dots, 4.5 arc minute gaps, a 30% dropout rate, and 6 gray levels.

The average correct response time provides a

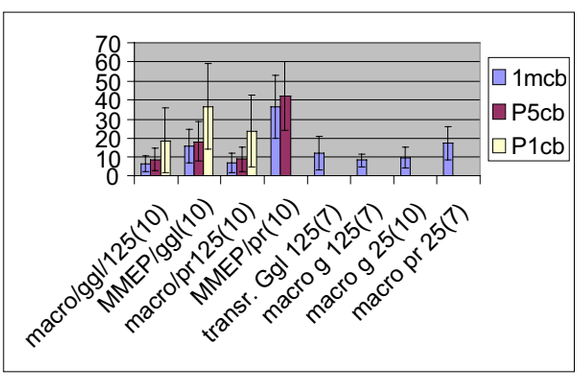


**FIGURE 13**

Threshold in microamps (y axis) with respect to electrode size and positioning on retina (x axis). Threshold currents are shown for 3 different pulse widths: 1 mcb = 1 ms cathodic first biphasic; P5cb = 0.5 ms cathodic first biphasic; P1cb = 0.1 ms cathodic first biphasic. Macro/ggl/125 = 125µ diameter. macroelectrode positioned on ganglion cell side; MMEP/ggl = MMEP electrode (20µ diameter) positioned on ganglion cell side; macro/pr125, 125µ diameter macroelectrode positioned on photoreceptor side; MMEP/pr = MMEP electrode (20µ diameter) positioned on photoreceptor side; transr Ggl 125 = transretinal electrode configuration with 125µ diameter electrodes; macro g 125, macro g 25, macro pr 25 = 125µ diameter electrode positioned on ganglion cell side, 25µ diameter electrode positioned on ganglion cell side, 25µ diameter electrode positioned on photoreceptor side, respectively. Numbers with each abbreviation on x axis are number of animals from which recordings were made.

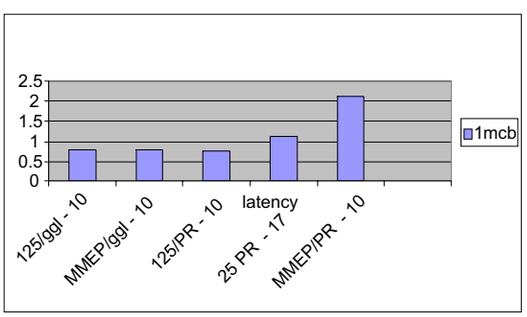


**FIGURE 14**

Latency in ms (y axis) using a pulse of 1 ms cathodic first biphasic pulse (1 mcb). 125/ggl = 125µ diameter electrode positioned on ganglion cell side; MMEP/ggl = MMEP (20µ diameter) electrodes placed on ganglion cell side; 125/PR = 125µ diameter electrode positioned on photoreceptor side; 25 PR = 25µ diameter electrode positioned on photoreceptor side; MMEP/PR = MMEP (20µ diameter) electrode positioned on photoreceptor side. Numbers with each abbreviation on x axis are number of animals from which recordings were made.

Mark, Thesis 11/9/01 11:29 AM Page 286



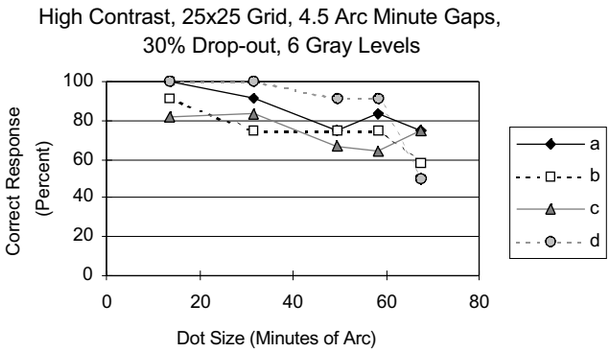


**FIGURE 15**
Decline in correct facial recognition as dot size increases. Data are from 4 subjects labeled a, b, c, and d.

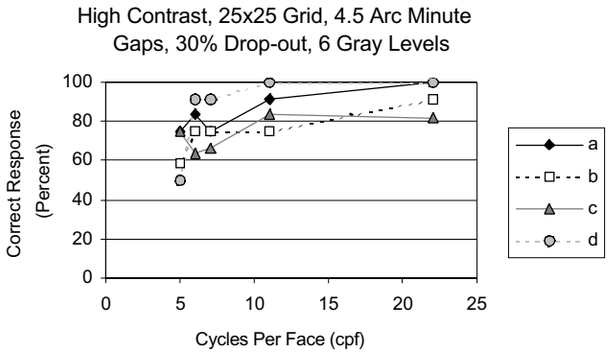


**FIGURE 16**
Decrease in facial recognition as a function of cycles per face. Data are from 4 subjects labeled a, b, c, and d.

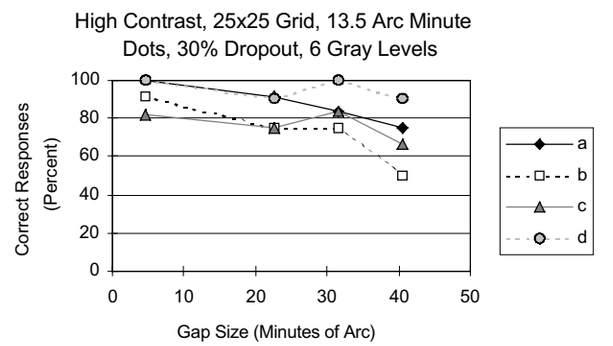


**FIGURE 17**
Effect of dot spacing on facial recognition. Data are from 4 different subjects labeled a, b, c, and d.

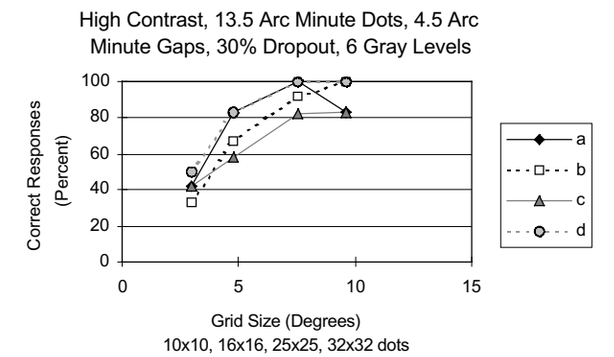


**FIGURE 18**
Effect of 6 levels of gray scaling on facial recognition. Data are from 4 subjects labeled a, b, c, and d.

measure of the analysis necessary to identify the face under evaluation (Fig 19).

An identification index was created as a measure of the speed and accuracy of the subject's responses under various testing conditions. The score is calculated by first squaring the percentage of correct responses and then subtracting the square of the number 50 from this value. The result is then divided by the average number of seconds required for a correct response. Thus, a positive score results when the subject identifies over half of the images correctly. Rapid responses also result in higher scores when the subject is able to identify the faces over 50% of the time. Recognition rates of less than 50% result in negative scores. To exceed an identification index of 1,000, a subject correctly identifying 80% of the faces correctly would need to do so with an average correct response time of less than 4 seconds.

Only 6 testing conditions yielded an average identification index score greater than 1,000. In all cases with an average identification index greater than 1,000, the gap size was 3.5 arc minutes and the resolution was 6 gray levels. In the high-contrast tests, grid sizes were at least 25 x 25 and the dropout rate was 30% or less with dot sizes of 13.5 arc minutes or 31.5 arc minutes. In the low-contrast cases in which the average identification index was greater than 1,000, the dot size did not exceed 13.5 arc minutes and the grid size was 32 x 32 with a 30% dropout rate, or 25 x 25 with a 10% dropout rate.

### *2.2 Letter/Symbol Recognition and Activities of Daily Living*

The Tumbling E Test showed that when using a 4 x 4 array, 87% of subjects could determine orientation of E at 10 cm (Fig 20). This corresponds with a Snellen acuity of 20/1810 (see Appendix for calculation of acuity). Using a 6 x 10 array, 87% of subjects could determine orientation of E at 30 cm, which corresponds with a Snellen acuity of 20/1330. Using a 16 x 16 array, 75% determined orientation at 70 cm. This is equivalent to a Snellen acuity of 20/420.

Results of the object recognition task are shown in Fig 21.

With the candy pouring task, many subjects touched 1 cup to the other just before pouring the candy, despite taking measures to avoid contact. Therefore, the data reflect both visual and tactile information (Table I).

Results for 7 of 8 subjects performing the cutting task

Mark, Thesis 11/9/01 11:29 AM Page 287



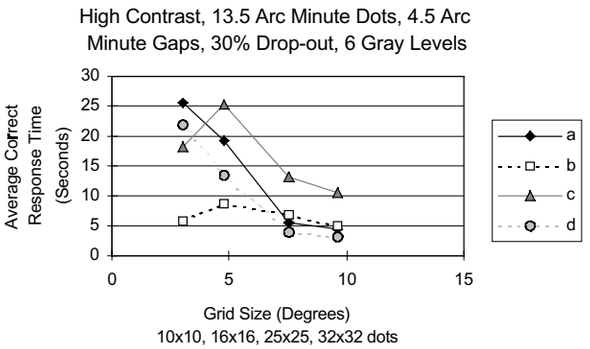


**FIGURE 19**
Average correct response time to identify a face. Data are from 4 subjects labeled a, b, c, and d.

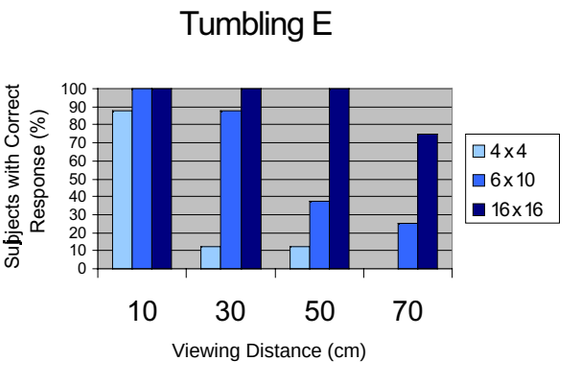


**FIGURE 20**
Correct percentage of responses during a Tumbling E Test using different sized pixel arrays as a function of viewing distance.

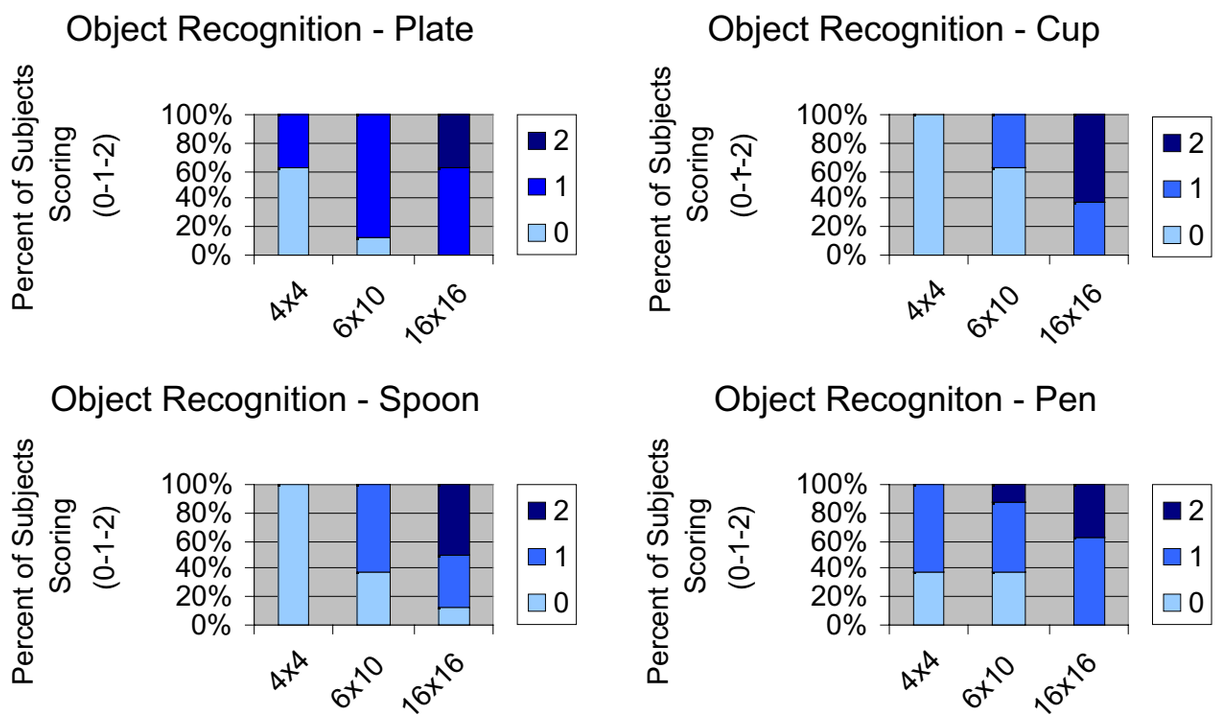


**FIGURE 21**
Object recognition using different number of pixel arrays. A score of zero was given for incorrect answer, a score of 1 for correct description but not exactly identifying the object, and a score of 2 for exact object recognition.

are shown in Fig 22. These 7 subjects used only visual information to cut the target object. The subject who was omitted from the results folded the paper to create a tactile target for cutting. His accuracy and cutting time were much higher than those of the other subjects.

Results of the symbol recognition task are shown in Fig 23.

In the reading test, only 3 of the 8 subjects using a 6 x 10 array could read the first sentence on the Minnesota Reading Card, which has a 72-point font (Fig 24). They correctly identified all 10 words with an average reading speed of 1.06 words per minute. Using a 16 x 16 array, all subjects were able to read all 10 to 12 words of both the first line of the Minnesota Reading Card (smallest font size, 72) as well as the first 5 sentences (smallest font size, 57). Using the same 16 x 16 array, all subjects read all 10 words of a 45-point font except 1 who read only 6 words. All subjects using the same array could read all 10 words of 36-point font except 1 who read only 8 words). When the point font was further reduced to 27, only 2 subjects read all 11 words, 1 subject read 5 words, and 1 subject read 4 words, 2 subjects read 3 words, 1 subject read 2 words, and 1 subject

Mark, Thesis 11/9/01 11:29 AM Page 288



TABLE I: NUMBER OF CANDIES SUCCESSFULLY POURED INTO A CUP IN 10 TRIALS

| SUBJECT NO. | NO. OF CANDIES POURED | | |
|---|---|---|---|
| | PIXEL NUMBER ARRAY | | |
| | 4x4 | 6x10 | 16x16 |
| 1 | 10 | 10 | 8 |
| 2 | 0 | 10 | 10 |
| 3 | 10 | 7 | 10 |
| 4 | 0 | 0 | 10 |
| 5 | 10 | 10 | 10 |
| 6 | 10 | 9 | 10 |
| 7 | 7 | 6 | 10 |
| 8 | 1 | 10 | 10 |

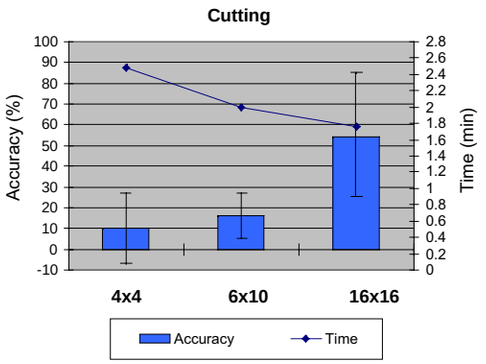


FIGURE 22

Percent accuracy and time to do cutting are represented as a function of different number of pixel arrays. Error bars represent standard deviation.

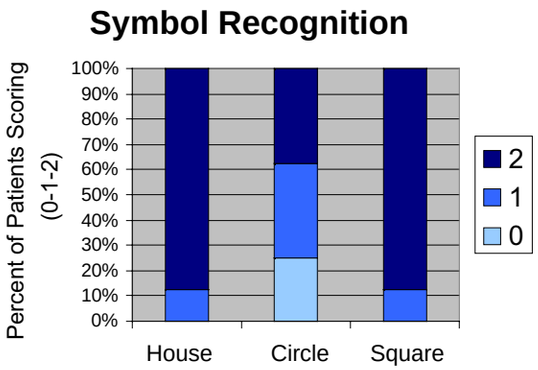


FIGURE 23

With a 4 x 4 pixel array, subjects scanned over three symbols on a Light House Key Card. Correct responses ("house," "circle," "square") were awarded 2 points, close responses were awarded 1 point, and inaccurate responses were awarded no points.

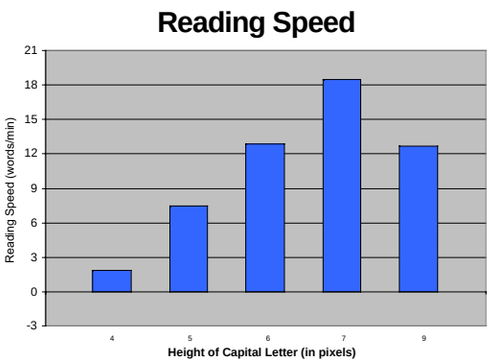


FIGURE 24

Reading speeds as a function of letter height.

read 0 words. One subject complained of motion sickness while viewing the scanning letters. This was the same subject who read 6 words on the 45-point font, 8 words on the 36-point font, and 0 words on the 27-point font.

Most subjects (87%) were able to read the 36-point font. The capital letter had a height of 0.8 cm. Reading this at a distance of 4.5 cm corresponds to a visual acuity of 20/600 with the 16 x 16 array.

## DISCUSSION

### 1. ELECTRICAL STIMULATION OF NEURONS

*1.1 Physiology of Neuron Excitation*

In 1939, it was found that during the propagation of an action potential in the giant axon of a squid, the conductance of the membrane to ions increased dramatically.[129] Subsequently, during the early 1950s, the first complete description of the ionic mechanisms underlying the action potential was proposed.[130,131] Electrical stimulation elicits a neural response by opening the voltage-sensitive ion channels, bypassing the chemically gated channels in the stimulated cell. Neuronal excitation threshold is the minimum electrical stimulus amplitude and duration required for initiating an action potential. Once the membrane reaches a certain potential, a trigger mechanism is released and an action potential results (all-or-none mechanism). Many of the studies designed to explore safe and effective parameters of electrical stimulation were based on extracellular recording of such action potentials.

Similarly, early experiments showed that secondary slow-wave retinal potentials have been induced by transretinal electrical stimulation of an amphibian eyecup preparation.[132,133] However, it should be noted that in the retina (photoreceptor, bipolar and horizontal cells) and probably in other parts of the central nervous system, there are neurons that, when excited, do not generate action potentials but only graded potentials.[133] In these neurons, electrical stimulation can evoke a graded potential that can be very difficult to document with extracellular recordings.

Mark, Thesis 11/9/01 11:29 AM Page 289



A number of factors can influence the efficacy of electrical stimulation. First, the threshold depends on the electrical properties and anatomy of the target neural elements, and what portion of the cell (dendrite, cell body, and axon) is stimulated. For example, because RGC axons are unmyelinated and of a small diameter, they are difficult to excite. Consequently, one computational model of extracellular field stimulation of the RGC has shown that even though the axon is closer to the epiretinal stimulating electrode, the extracellular stimulation threshold of the RGC soma is 58% to 73% lower than its axon.[134]

Second, the threshold is obviously affected by the distance from the electrodes to the target cell. However, there can be an inhibitory effect from the stimulation. For example, for myelinated axons, it has been shown that those axons very close (<500 μm) to the electrode may not be stimulated because of current flow considerations.[135] Third, the threshold is also affected by inter-electrode separation as well as the PD.[134,136] Fourth, threshold can vary significantly owing to the impedance of tissues, and errors can be associated with the assumption that tissue electrical properties are the same in every stimulated compartment (isotropic tissue properties), especially with bipolar electrical stimulation.[137]

Fifth, there is a well-defined relationship between the threshold current/charge and stimulus PD required for neuronal activation.[138-140] As the PD decreases, the threshold current increases. This relationship begins to break down at the extremes (ie, a very short current pulse cannot activate a nerve regardless of the amplitude). Similarly, as the PD increases, the threshold current approaches a minimum value called the rheobase, below which an action potential cannot be elicited regardless of PD. A chronaxie is the pulse width for which the threshold current is twice the rheobase current.[135] Charge, which accounts for both the pulse amplitude and PD, is probably the most meaningful parameter for the electronic prosthesis. This is because electrode metals can withstand only certain charge density before irreversible toxic reactions occur at the electrode tissue interface.

Sixth, in addition to current amplitude, charge, and PD, investigators found that threshold is affected by the frequency of stimuli.[32,52] In one of the experiments, the threshold was constant at frequencies of 150 to 200 Hz and increased 50% at 75Hz.[32] Furthermore, it was found that only those pulses delivered in the first 100 ms would determine the sensory response for trains of stimulus pulses at any specified set of parametric values.[29]

Seventh, the polarity of electrical stimulation is also an important factor. Neurons can be activated by cathodic threshold activation, anodic pulses, and biphasic pulses.[141-144] In many neural systems, higher currents were required to reach threshold with anodic stimulation compared to cathodic stimulation, so cathodic stimulation is considered the preferred polarity for most of the visual prostheses.[135] Biphasic waveform can have either a cathodic or anodic wave first. However, for most applications, cathodic first biphasic pulses have resulted in the lowest thresholds.[56,88,145] The 2 phases of the biphasic pulse are used for charge balancing and thus avoiding irreversible reactions at the tissue electrode interface, which in its extensive form can result in electrolysis and significant pH changes as well as electrode metal deposition into tissue. The 2 phases can have equal amplitudes and PD but can also be asymmetric, with 1 of the phases having a lower amplitude but large duration in order to result in charge balance. Asymmetric charge-balanced biphasic waveforms were discovered to increase the reversible charge injection limits.[142] However, to date, in a series of patients that underwent retinal electrical stimulation, there was no difference between monopolar versus bipolar stimulation and cathodic versus anodic first stimulation.[47]

Eighth, another variable for threshold stimulation is the waveform. There are 2 basic waveforms for neural stimulation: sinusoidal and pulsatile (square) waveforms. There are many variants of these basic waveforms that can be used for different purposes. Experiments that were performed to examine the question of the optimal stimulation waveform showed that a pulsatile (square) waveform has the lowest threshold. The different threshold values found for electrical stimulation of several points along the visual pathways are presented in Tables II and III.

It should be noted that these studies were performed in different species, at different electrophysiological sites, using different electrode sizes, and with different stimulus parameters (eg, pulse frequency, PD, waveforms, pulse trains). The threshold measured is either physiological (recording evoked potentials or single neuron responses from RGC or primary visual cortex neurons) or by measuring psychophysical responses (phosphene perception or behavioral reaction in monkeys[144]). Thus, these results can give only an estimate of electrical stimulation threshold values of various locations along the visual system, and only a few conclusions can be drawn as to the methods to be used during electrical stimulation. It is clear that the psychophysical threshold for intracortical microstimulation[26,32,33] is lower than the threshold of surface cortical stimulation. In addition, the in vitro electrophysiologic threshold is lower than the in vivo electrophysiologic and psychophysical thresholds.[47,54,58,143,144,146] This discrepancy is maybe due to the fact that the visual system cannot recognize a single RGC action potential. If this is the case, the exact number of stimulated RGCs for in vivo psychophysical thresholds should be determined.

Typical charge density threshold values (0.16 to 70 $mC/cm^2$) for retinal stimulation of patients with RP were

Mark, Thesis 11/9/01 11:29 AM Page 290



**TABLE II: THRESHOLD PARAMETERS FOR DIFFERENT TYPES OF VISUAL PROSTHESES**

| CORTICAL SURFACE STIMULATION | INTRACORTICAL MICROSTIMULATION | EPIRETINAL STIMULATION | SUBRETINAL STIMULATION | OPTIC NERVE STIMULATION |
|---|---|---|---|---|
| Blind glaucoma patient, 4 mA, 200 μsec, 100 Hz, electrode diameter 0.8 mm, charge density 159 μC/cm²/pulse[19] | Macaques, current threshold 1-5 μA, electrode surface area $0.3^{-1}.6x10^{-3}$ mm², charge density threshold 100-1,800 μC/cm² [144] | Rabbits, extradural recording, threshold current 105-720 μA, PD 100 μsec, electrode diameter 40 μm, charge density threshold 0.8-5.7 mC/cm² [60] | Normal rabbits (cortical recordings), electrode surface area 0.36 cm², charge density threshold 2.8-100 nC/cm² [63] | RP patient, threshold current 30 μA, PD 400 μsec, electrode area 0.2 mm², frequency 160 Hz, charge density threshold 24 μC/cm²/pulse [52] |
| Blind human-optic atrophy, 620 μA, 0.1 msec 120 Hz 1 mm electrodes, charge density 7.9 μC/cm²/pulse[18] | Epileptic patients, current threshold 20-200 μA, electrode surface area 200 μm², PD 0.4 msec, frequency 100 Hz, train length 0.1-1 sec, charge density 3.9-39 mC/cm² [25] | RP and AMD patients, threshold current 500 μA, PD 2 msec PD, charge density threshold 0.16-70 mC/cm², (1μC/phase)[47] | | |
| Normal sighted patients, 0.25-1 mm diameter Pt electrodes, 0.5 msec PD, 60-120 Hz, 1 mA[21], charge density 63-1,000 μC/cm². | Blind glaucoma patient, threshold current 1.9-25 μA, PD 200 μsec, electrodes surface area 200 μm², charge density 0.2-2.4 mC/cm² [32] | Laser treated human retinas, threshold current 100-600 μA, 0.1-0.6 μC, 0.8-4.8 mC/cm² [153] | | |
| Cats, PD 0.5 sec, frequency 60/120 Hz, trains up to 4 sec, current threshold 1-3 mA, electrode surface area $0.5\text{-}2x10^{-3}$, charge density threshold 25-4,000 μC/cm² [21] | Cats, auditory behavioral task, charge threshold - 8.9 nC/phase, charge density threshold ~18 mC/cm² [33] | Normal mice, 0.055 μC, 455 μC/cm2, 16-week-old rd mice - 0.075 μC, 621 μC/cm² electrode diameter 125 μm, PD 0.08 msec [55] | | |
| Human subjects. Current threshold 0.79-3.50 mA (average 1.76 mA), train 0.5 sec, PD 0.25 msec, electrodes surface area 1-2mm², charge density threshold 22-44 μC/cm²/pulse[28] | | Normal mice, threshold current 240 μA, threshold charge density 1.9 μC/cm², rd mice 592 μA, charge density 4.8 μC/cm², electrode diameter 125 μm, PD 1 msec[56] | | |
| Human subject, frequency 30 Hz, 1-50 pulses, PD 0.5 msec, voltage threshold 10-20 volts, no impedance reported[30] | | Normal human subject, 19 μC/cm² (12 μA, PD 2 msec, electrode diameter 400 μm). RP patient, 0.3 mC/cm², (1.5 mA, PD 0.25 msec, electrode diameter 400 μm[58] | | |

AMD, age-related macular degeneration; PD, pulse duration; Pt, platinum; RP, retinitis pigmentosa.

well above the safe threshold for platinum electrodes chronic stimulation.[54] Other investigators reported comparable threshold values recently (0.3 mC/cm² in a patient with RP).[58] These values are affected by the fact that many times the stimulating electrodes were as far as 0.5 mm from the retinal surface. Nevertheless, one cannot exclude the fact that the degenerated retina may require higher charge. If the charge requirements are higher because of the relative degeneration of the retina, then for these patients with more degenerated retinas, the electrodes sizes will have to be larger in order to reduce the charge density and keep it within safe limits for long-term stimulation.

### *1.2 In Vitro Retinal Experiments*

A limited number of in vitro experiments to define threshold

Mark, Thesis 11/9/01 11:29 AM Page 291



**TABLE III: THRESHOLD PARAMETERS FOR EPIRETINAL VERSUS SUBRETINAL PROSTHESES**

| EPIRETINAL STIMULATION | SUBRETINAL STIMULATION |
|---|---|
| Pt electrodes.<br>2.98 μC/cm2 (bullfrog). 8.92 μC/cm² (normal rabbit).<br>11.9 μC/cm² (chemically RD rabbit).[46] | Chick isolated retina. 35 μA PD 0.4 msec, electrode surface area 0.01 mm², charge threshold 14 nC/phase, charge density threshold 178 μC/cm².[146] |
| Human isolated retina. Electrode diameter 10 μm, PD 400 μsec, threshold current, 0.18 μA- 0.52 μA, threshold charge density 91-264 μC/cm².[149] | Retinal degenerate rats (RCS) isolated retina. Threshold charge density 500 μC cm².[149] |
| Rabbit isolated retina, 51.85 μC/cm² (ganglion side stimulation) vs. 55.35 μC/cm² (photo receptor side), PD 1 msec.[143] | |

currents for retinal electrical stimulation have been performed in different preparations. One study of normal retinal stimulation was performed in bullfrog eyecups and reported a charge threshold of 3.75 nC with biphasic square current pulses of 75 msec/half phase.[147] Another study was performed with normal human isolated retinas. These retinas came from normal subjects submitted to enucleation on account of orbital cancer. Charge density threshold values were between 91 μC/cm² and 264 μC/cm². These results were similar to findings in isolated rabbit retinas, concluding that rabbits are a good model to study retinal electrical stimulation.[143,145,148]

Reported in this thesis are our electrical stimulation results from rabbit retinal isolate. Threshold parameters during various in vitro electrical stimulation experiments, including from this thesis, are shown in Table III. Among the parameters tested were the electrode position (ganglion or photoreceptor cell side) and the stimulating electrode size (10, 25, 125 μm diameter). It was shown that the charge density threshold for stimulation from the ganglion side is lower (51.85 μC/cm²) than from the photoreceptor side (55.35 μC/cm²), especially when using 125 μm diameter electrodes. Other investigators have obtained even lower thresholds (0.4 nC) when stimulating from the photoreceptor side.[146]

One study that was performed on isolated retinas from retinal degenerate rats[150] reported a threshold charge density of 500 μC/cm². Again, we can see that a much higher-charge density threshold is required to stimulate diseased retinas, similar to in vivo experiments. Given that stimulation thresholds change depending on the health of the retina, future experiments need to study and compare stimulation thresholds between normal and retinal degenerate retinas.

*1.3 In Vivo Experiments*

Since many of the experiments prior to a safe and effective implantation in humans have been and will be performed in animals, methods of recording the function of the central visual system have been developed. Threshold parameters during various in vivo electrical stimulation experiments are shown in Table II.

Several experiments using scalp and subdermal electrodes positioned over the visual cortex were performed to conclude that electrical evoked responses (EER) can be recorded after external electrical stimulation of the eye.[37-39,45,63,116,151,152] In one of the studies, it was discovered that the EER stimulation threshold was significantly increased for advanced retinal degenerate dogs (RCD1) versus normal dogs (4 mA versus 1.1 mA, $P < .05$).[57]

Penetrating electrodes within the cortical tissue have the potential to record single neuron activity in addition to multiunit activity recorded by epidural electrodes.[35,152] One of the studies involved normal and retinal degenerate (rd) mice. Single cortical neuron response to retinal electrical stimulation showed dose-dependant effect, and similar to other studies, the current amplitude threshold was significantly lower for normal mice (240 μA) versus rd mice (592 μA, $P = .001$).56

Other invasive methods for recording visual evoked potentials have also been studied. In vivo retinal stimulation with an epiretinal microfilm electrode array was performed in normal cats with recording of the responses from the visual cortex being performed with epidural recording electrodes. The charge balanced threshold value was 178 μC/cm.[21,46] Subdural electrodes were also used recently to record visual and electrical evoked potentials and proved to have lower thresholds than subdermal electrodes.[152]

In the experiments reported in this thesis, responses for electrical stimulation of the eye were recorded from ganglion cells in the same stimulated eye. Normal mice were compared to rd mice of different ages in regard to electrical stimulation threshold. A 1-kHz sinusoidal waveform was more efficient than a biphasic current pulse of 500 μs/phase in normal mice, but in the 2 rd-mice groups, threshold charge was not dependent on waveform shape. RD mouse retina is almost completely absent of

Mark, Thesis 11/9/01 11:29 AM Page 292



photoreceptors, but the inner retina (bipolar cells and retinal ganglion cells) is less affected. This suggests that the sinusoidal waveform is more suitable to stimulate the photoreceptor cells, but there is no difference between sinusoidal waveform and square waveform when stimulating the inner retina. Pulse trains were tested to determine if a series of pulses would "appear continuous" to the retinal cells and thereby use less charge to elicit a response. The opposite was found to be the case. A train of 5 x 40-μs/phase pulses (where the pulse train lasted for 0.6 ms) required 2 to 3 times as much current as a continuous 0.5-ms pulse, meaning the cells did not respond to the train of short pulses as if it was a single long pulse. In fact, the current threshold for the pulse train was only slightly lower than a single 40-μs pulse.

The excitation threshold was significantly higher for 16-week-old rd mice versus normal mice (0.075 versus 0.055 μC for 0.08-ms square pulse, $P < .05$). This is most likely due to the more degenerated inner retina requiring more current to excite it. The number of intact inner retinal cells in an 8-week-old mouse retina is more than that of a 16-week-old mouse retina. This result correlates well with data obtained from short-term electrical stimulation tests in humans, in which it was demonstrated that areas of more severe retinal damage, either from RP or laser damage, had a higher electrical stimulus threshold.[153]

In all mice groups, short-duration pulses (40, 80, and 120 μs) were more efficient in terms of total charge than longer pulses (500 and 1000 μs). However, because the current pulses are so short, a relatively large current is required to reach threshold. Electronics capable of delivering high current, even for a short time, may be difficult to implement in a design that is efficient in terms of size and power consumption. Moreover, longer pulses may also preferentially target the bipolar cell layer and therefore possibly make use of more of the inner retinal neuronal function.[115] The pulse threshold data can also be used to design a retinal stimulating array. Each individual stimulating electrode within the array must be designed such that it can safely supply the appropriate level of stimulating current to the retina. The design considerations are electrode material and electrode size. Assuming a planar, platinum disc electrode, the diameter of this electrode would have to be 170 μm to support 0.07 μC (the threshold charge in 8-week rd mouse with a 0.5 ms pulse). This assumes a safe chronic stimulation limit of 0.1 $mC/cm^2$ for platinum. As the precise technology to be used for the retinal prosthesis becomes clear, neural response data like that reported here will be essential to the development of the final device.

*1.4 Future Studies in Electrophysiology*

Future studies are needed to identify the target cell for retinal electrical stimulation. The thickness of the nerve fiber and the ganglion cell layers is at least 20 to 200 and 20 to 40 μm, respectively. Thus, an epiretinal implant places the stimulating electrodes at quite a distance from the desired target of signal initiation (ie, the ganglion or the bipolar cell layers). Since there is a 3-dB rise in threshold for every 250 μm,[115] more current will be necessary for electrical stimulation. Stimulating the bipolar cells could allow for more of the natural retinal processing to take place. Stimulating the ganglion cells, which are closer to the epiretinal electrode array, may require less current but could require more image processing and complex stimulation patterns to account for the lost retinal processing.

The cell bodies (somas) of these ganglion cells are mapped over the surface of the retina in a manner that approximates the projection of the visual world onto the surface of the retina. However, at any particular location on the surface of the retina, axons from peripheral sites course over the individual ganglion cell bodies. If these superficial passing axons were preferentially stimulated, groups of ganglion cells from large areas of the retina would be excited. One might expect the visual perception of such a stimulus to appear as a wedge or arc because of the characteristic course of the ganglion cell axons in the nerve fiber layer. On the other hand, if the ganglion cell bodies or deeper retinal cells were stimulated, one would expect the visual perceptions to be focal spots.

Early experiments showed that inner retinal layers can be electrically stimulated and elicit an EER.[132,154] It has also been shown that phosphenes elicited by electrical stimulation over a krypton laser scar (causing outer retinal damage) best simulated the visual perceptions previously reported due to electric stimulation in blind RP and AMD patients, suggesting that the site of electric stimulation in those patients is the inner retina.[153] These results, although suggestive, have not determined the exact target cell for retinal electrical stimulation.

Another line of evidence came from electrical stimulation of the retinas of patients with RP or AMD. When stimulated with platinum disc electrodes 50 to 200 μm in diameter, the patients reported spots of light and not wedges.[47,54,58] This would implicate that the electrodes did not preferentially stimulate the RCG axons.

Additionally, circumstantial evidence suggesting that retinal bipolar cells may be the target for retinal electrical stimulation comes from postmortem morphometric analysis of the retinas of both RP and AMD patients. This analysis has shown that there were many more bipolar cells left compared to RGCs in the retinas of these patients.

Recently, latency experiments that were conducted in isolated frog retinas showed that higher currents stimulate RGCs directly, while lower currents activate other cells

Mark, Thesis 11/9/01 11:29 AM Page 293



(photoreceptors, bipolar cells).[115] Another finding was that the target cells of shorter PD (<0.5 ms) were RGC cells/axons, whereas a deeper cellular element was the target for longer PD (>0.5 ms). This is consistent with the finding that deeper retinal cells have unusually long chronaxies compared to RGCs.[115]

In conclusion, there are several lines of evidence to suggest that epiretinal electrical stimulation of the retina can result in well defined retinotopic visual percepts. To get such phosphenes one should avoid RGC axonal stimulation and probably activate bipolar cells by varying stimulation parameters.

## 2. PSYCHOPHYSICAL EXPERIMENTS

In an effort to define the minimum acceptable resolution for useful vision, several psychophysical experiments were performed. As early as 1965, it was suggested that 600 channels, or points of stimulation, would be sufficient for reading ordinary print.[155] Others suggested that 80 to 120 points (pixels) are sufficient for large-print reading, while 200 points may allow recognition of simple obstacles.[156]

More recent studies of simulated pixelized vision showed that 625 points of stimulation is a better estimate for useful vision.[157-159] These studies were conducted with a portable "phosphene" simulator, which consisted of a small head-mounted video camera and monitor worn by a normally sighted human subject. To simulate a discrete phosphene field, an opaque perforated film masked the monitor. The visual angle subtended by images from the masked monitor was 1.7° or less, depending on the mask, and fell within the fovea of the subject. It was concluded that 625 electrodes implanted in a 1-$cm^2$ area near the foveal representation of the visual cortex could produce a phosphene image with a visual acuity of approximately 20/30. Such acuity could provide useful restoration of functional vision for the profoundly blind.[159]

In another experiment, in which the same methods were used, the reading speed was measured in subjects viewing pixelized text. The results indicated that a 25 x 25 pixel array representing 4 letters of text is sufficient to provide reading rates near 170 words per minute with scrolled text, and near 100 words per minute with fixed text.[158]

The feasibility of achieving visually guided mobility was investigated with a similar device. Normally sighted human subjects were required to walk through a maze that included a series of obstacles. The results indicated again that 625 pixels provided useful visually guided mobility. Walking speed increased fivefold during 3 weeks of training.[157]

To make a cortical electrode array of 600 or more channels, several methods were proposed. Considering the visual cortex mean extent of 9.7 $cm^2$, the number of penetrating electrodes that can be inserted, using current technologies, can reach 10,000 or more.[128]

Although these studies began to delineate the number of electrodes needed, the fact that all the pixels were projected on a very small area of the retina made it impractical to translate to the design of the retinal prosthesis, in which the electrodes would be spread over the entire macular region. The results from experimentation presented in this thesis address this shortcoming by projecting the pixels over the entire macular region. With our setup face recognition, reading speeds as well as certain activities of daily living were tested.

### *2.1 Face Recognition and Reading Speed*

This simulation indicates that rapid and accurate facial recognition can be achieved by using pixelized dot images. The performance was maximized when the pixelized grid was at least 25 x 25 dots in size with 6 levels of gray-scale resolution. Excellent speed and accuracy were achieved with dot sizes of 13.5 arc minutes, gap sizes of 4.5 arc minutes, and dropout rates of 30% or less. High-contrast images resulted in improved facial recognition rates. High facial recognition rates required sampling the facial images at eight or more cycles per face. An increased concentration of dots per character resulted in increased reading speed. As the frequency of dots approaches the Nyquist limit, reading speed decreased dramatically. A larger grid area also improved reading speed. A grid size of 7° is acceptable, but marked improvement was noted with a grid size of 10°.

This simulation of pixelized prosthetic vision suggests that prosthetic visual devices designed to the specifications above may be capable of providing individuals with visual perceptions that would enable a high facial recognition rate and adequate large-print reading speeds. Specifically, a fair level of visual function can be achieved with pixelized vision using a 16 x 16 grid encompassing a 10° field, high-contrast imaging, and 4 or more gray levels. Simulation studies such as this will help to further establish design criteria to maximize the performance of such implants.

### *2.2 Letter/Symbol Recognition and Activities of Daily Living*

One of the most important findings of these experiments was the impact of being able to scan. Even with a very rudimentary electrode array of 4 x 4, 87% of the subjects could correctly identify a tumbling E. Certainly, with 16 x 16 electrodes, most of the subjects could even perform complex tasks such as object recognition and cutting. The impressive ability to perform with such a limited number of pixels in lieu of the fact that we have 100 million, if not more, photoreceptors bodes well for the development of

Mark, Thesis 11/9/01 11:29 AM Page 294



a retinal prosthesis. If the electronic implant had to stimulate the retina in millions of points, this would be impossible owing to the extreme amounts of power requirements and heat dissipation that would irreversibly damage the retina. However, electrode technology and stimulation parameters more than likely could result in a retinal prosthesis with 16 x 16 electrodes placed over the macular region.

The small number of pixels needed to perform complex tasks should not be a total surprise. Albeit, a different sensory system, clinical experience with the cochlear implant has demonstrated that electrical stimulation with as few as 4 to 8 input channels allows patients to talk over the phone. Perhaps a similar phenomenon (redundancy in visual information) and the plasticity of the visual cortex will permit fewer retinal stimulating electrodes to give blind patients some useful vision.

However, the result from these psychophysical tests does need to be taken in its context. The electrical stimulation to produce phosphenes at the retinal level is undoubtedly going to stimulate groups of neurons in a manner very different than how light pixels stimulate the normal retina. Thus, the definitive answer to the number of electrodes or pixels needed to be generated by an electronic device still will be determined when blind patients are fitted with these implants and allowed to use them in their activities of daily living.

### *2.3 Future Studies*

Future studies may investigate the parameters necessary for pixelized vision to provide the sufficient visual information for individuals to independently perform activities of daily living (ADLs). Such survival tasks may include eating, self-care (health care and personal hygiene), communicating with others, and independent mobility. Another method of assessing visual function includes the ability to perform more complex visually guided tasks, known as instrumental activities of daily living ([I]ADLs) such as managing personal finances, shopping, and housekeeping.

Future simulation studies may also evaluate the impact of frame rates less than 30 Hz and flicker. Additionally, the effect of image enhancement may also be investigated. Such studies may examine the effects of edge detection, high pass filtering, black-white image reversal, and magnification.

## 3. SUMMARY

The 3 levels of hierarchy in the sensory systems (namely, receptor organ, sensory pathways, and perception) suggest a similar architecture for artificial sensory systems. Accordingly, artificial systems should include a transducer corresponding to the receptor organ, an encoder corresponding to the sensory processing system, and finally an interpreter corresponding to perceptual functions. In other words, the visual environment is captured and processed by a photosensing device such as a digital camera, and the pixelized information is transmitted to a stimulating electronic chip. This chip, in turn, activates a penetrating electrode array with a pixelized pattern that allows the patient to correctly see the image.

The epiretinal implant is designed to have 2 units, 1 extraocular and 1 intraocular. Previously, a visual intraocular prosthetic chip including a photosensor, processor, and a stimulus-driving chip was developed.[160] However, it became apparent that an improvement could be achieved in having photosensing[161] or video capture performed extraocularly. This modification would allow for enhanced videoprocessing, more custom control over the video signal, and less hardware to be implanted into the eye. The 2 units are connected by either a modulated laser[51] or an inductive link,[106] allowing the intraocular unit to derive both power and data signals from the extraocular unit. The extraocular unit includes a video camera and a video processing board, a telemetry/laser protocol encoder chip, a radio frequency amplifier, and a primary coil (or laser source). The intraocular unit consists of a secondary coil, a rectifier and regulator, a retinal stimulator with a telemetry protocol decoder, a stimulus signal generator, and an electrode array.

The subretinal approach uses direct visible and infrared light. The stimulation power is then locally enabled by an amorphous silicon photoconductor, according to the image projected onto the device by the optical system of the eye. The photodiodes, in turn, activate adjacent electrodes, which stimulate the bipolar/ganglion cells above them.[48,49]

Many of the electronic components of the cortical prosthesis system should be similar to those of the retinal prosthesis. However, the cortical prosthesis will also need a complex real-time algorithm to map the visual information correctly onto the cortex via microelectrodes. One of the cortical prosthesis groups still uses a connecting "pedestal" that perforates the scalp and links the processing computer with the electrode array. This pedestal allows the passage of wires through the skin.[23,26] With current technologies, it might be possible to miniaturize the electronics and use wireless connections between the sensor and the stimulator to decrease the bulkiness of the device.

Attempts at implanting electronic devices at various parts along the visual pathways were discussed. Both major achievements and obstacles remaining were summarized. Given that intact neurons along the visual pathways can be found in almost all blind patients, it is only

Mark, Thesis 11/9/01 11:29 AM Page 295



our lack of understanding that prevents us from stimulating them in a safe and effective manner. We believe that as our knowledge increases about how to stimulate neurons with microelectronics and as microelectronics and material sciences continue to evolve, we should one day be able to restore vision to the blind. Given the advances that have been made in this field, we can only hope that the day such devices are widely used is in the near future and not decades away.

## APPENDIX

### 1. METHODS

*Pixelized Vision Simulator*

Several video camera adjustments were made to maximize contrast. Brightness was set at 131, contrast 255, cyan 0, yellow 0, saturation 74, video quality 0, and exposure time 128; light sensitivity was varied between 255 and 68.

*Sizing of Arrays*

This was done by first determining the percentage of visual field occupied by the active monitor displayed in the headset. Utilizing the "see-through" feature, the length of the active window image was measured in space at a fixed distance from the eye. Using simple trigonometry, the angle was found to be 28°. This number was correlated to the size of the active window on the PC monitor. It was found that a 7.6-cm image on the computer monitor created a 7.3° image displayed on the retinal surface. A template was made to use as a guide for manually resizing the display window on the computer monitor.

*Setup for First Set of Tasks*

The camera was focused appropriately for a 10- to 70-cm range. Video camera light sensitivity was set at 68 for these tasks in order to minimize a washout effect seen under the lights when the camera is mounted on the subject's head.

*Calculation of Expected Visual Acuity*

For a completely unambiguous identification of an E, each branch of the E must lie at the center of 2 noncontiguous pixels (2 center-to-center distances). A person with 20/20 vision can differentiate the images of 2 lines at 2 arc minutes apart on the retina. This can be expressed in the following equation:

$$\frac{X}{20} = \frac{2 \text{ center-to-center distances in the array}}{2 \text{ arc minutes}}$$

X is the new denominator in the Snellen acuity. Two center-to-center distances are 4° (240 arc minutes) for the 4 x 4 and 6 x 10 arrays and 1.6° (96 arc minutes) for the 16 x 16 array. This gives the expected visual acuities of 20/2400 for the 4 x 4 and 6 x 10 arrays and 20/865 for the 16 x 16 array.

*Tumbling E*

At each distance, subjects were encouraged to scan vertically and horizontally with the camera. Subjects were discouraged from guessing, and if they incorrectly identified the direction, the letter was rotated before the next attempt so that they still had all 4 options.

*Object Recognition*

For this task, the subjects were allowed to move the camera as close to the object as they desired. They were encouraged to look at it from a seated position as well as standing and looking directly down on it. They were also permitted to place their hand on the table without touching the object for the purpose of size comparison. Object 1 was a white plate 22.5 cm in diameter. Descriptions judged as accurate included circular, round, flat, and disklike. Descriptions judged as inaccurate included rectangular, plus-sign, and triangular. Object 2 was a white cup, 9 cm tall, 5 cm in diameter at its base, and 8 cm in diameter at its rim. Descriptions judged as accurate included wider top, thinner bottom, straight edges while seated, circular while standing over object. Descriptions judged as inaccurate included: square, rectangular, crosslike, and star-shaped. Object 3 was a white spoon, 14.5 cm long, with a 1.1-cm-wide handle and 4.1-cm-diameter head. Accurate descriptions were stop-sign shaped, straight line that is fuller on top, lollipop-like. Felt to be inaccurate were sticklike, rectangular, and crosslike. Object 4 was a white ink pen, 14 cm long and 0.7 cm thick. Accurate descriptions were long, thin, and sticklike. Judged as inaccurate were circular and an ill-defined shape.

*Candy Pour*

The cups were white, 9 cm tall, 5 cm in diameter at the base, and 8 cm in diameter at the rim. The candies were disc-shaped, 2.5 cm in diameter, and 0.8 cm thick. Subjects were asked to visually locate the 2 cups and encouraged to view them from different angles, including standing and looking directly down on them. The observer stabilized the cup as the subject began their pour.

*Cutting*

The sides of the rectangle were 2.6 cm thick, 15 cm long, and 14.6 cm wide. Subjects were given a pair of blunt-ended safety scissors in their dominant hand. A black cloth was held behind the sheet of paper to add more contrast. Subjects were encouraged to locate their hand and scissors before starting to cut.

Mark, Thesis 11/9/01 11:29 AM Page 296



*Setup for Second Set of Tasks*

The camera was refocused for this new distance. The light intensity setting was also increased to 255, which optimized the contrast at this distance. Subjects were briefly instructed on how to use the apparatus and were allowed to practice manually scanning the platform-mounted camera across sample reading material.

*Symbol Recognition*

Each symbol was a hollow black object with 0.6 cm thick lines. The first symbol tested represented a house and was 4.4 cm wide and 4.5 cm tall at the center. The second symbol was a circle with a 4.4 cm diameter. The last was a square measuring 4.4 cm per side. A close response for the house was "arrow." Close response for the circle was "oval," and that for the square was "rectangle.' Inaccurate response for the circle was "square" or "hexagon."

## 2. RESULTS

*Calculation of Actual Visual Acuity*

First we multiply the angle the letter would subtend on the retina (if it were viewed by the naked eye) by the magnification factor inherent in our system.

(2 arc tan 0.5h/d)° x y°/46° = Z°

where:

h= height of the letter

d= distance of camera lens from the letter

y= amount of retinal surface exposed to visual input

7.3° for 4 x 4 array

15.3° for 6 x 10 array

11.3° for 16 x 16 array

46°=visual field captured by the camera

Z= height of letter on retinal surface

Since we know the height of a 20/20 letter E subtends 5 arc minutes on the retina, it is possible to calculate visual acuity with our setup.

$$\frac{X}{20} = \frac{Z \times 60}{5 \text{ arc minutes}}$$

where:

X= the denominator in Snellen acuity

*Reading*

With a 6 x 10 array reading 72-point font, the height of the capital letter was 4 pixels. With a 16 x 16 array, the height of the capital letter in the 72-font sentence was 9 pixels. It was 7 pixels in the 57-point font, 6 in the 45-point font, 5 in the 36-point font, and 4 in the 27-point font. Subjects were encouraged to use the context of the sentence to help identify more difficult words.

## REFERENCES


1. Ross RD. Is perception of light useful to the blind patient? (Editorial and Comments) *Arch Ophthalmol* 1998;116:236-238.
2. Berson EL, Rosner B, Sandberg MA, et al. A randomized trial of vitamin A and vitamin E supplementation for retinitis. (Comments) *Arch Ophthalmol* 1993;111:761-772.
3. Sharma RK, Ehinger B. Management of hereditary retinal degenerations: present status and future directions. *Surv Ophthalmol* 1999;43:427-444.
4. del Cerro M, Gash DM, Rao GN, et al. Retinal transplants into the anterior chamber of the rat eye. *Neuroscience* 1987;21:707-723.
5. Galvani L. De viribus electricitatis in motu musculary, commentarius. *De Bononiensi Scientiarum etArtium Instituto atque Academia* 1791;7:363-418.
6. Fritsch G, Hitzig J. Ueber die elecktrische erregbarkeit des grosshirns. *Arch Anat Physiol* 1870;37:300-332.
7. Glenn W, Mauro E, Longo P, et al. Remote stimulation of the heart by radiofrequency transmission. *N Engl J Med* 1959;261:948.
8. Djourno A, Eyries C. Prothese auditive par excitation electrique a distance du nerf sensorial a l'aide d'un bobinage inclus a demeure. *Presse Med* 1957;35:14-17.
9. Buckett JR, Peckham PH, Thrope GB, et al. A flexible, portable system for neuromuscular stimulation in the paralyzed upper extremity. *IEEE Trans Biomed Eng* 1988;35:897-904.
10. Ziaie B, Nardin MD, Coghlan AR, et al. A single-channel implantable microstimulator for functional neuromuscular stimulation. *IEEE Trans Biomed Eng* 1997;44:2011.
11. Cameron T, Loeb GE, Peck RA, et al. Micromodular implants to provide electrical stimulation of paralyzed muscles and limbs. *IEEE Trans Biomed Eng* 1997;44:781-790.
12. Ledergerber CP. Postoperative electroanalgesia. *Obstet Gynecol* 1978;51:334-338.
13. Gross RE, Lozano AM. Advances in neurostimulation for movement disorders. *Neurol Res* 2000;22:247-258.
14. Foerster O. Beitrage zur Pathophysiologie der Sehbahn und der Spehsphare. *J Psychol Neurol* (Lpz) 1929;39:435-463.
15. Krause F, Schum H. Die epiliptischen Erkankungen. In: Kunter H, ed. *Neue Deutsche Shirurgie*. Stuttgart, Germany: 1931:chap 49a.
16. Penfield W, Rasmussen T. *The Cerebral Cortex of Man*. New York, NY: Macmillan;1952;135-147.
17. Penfield W, Jasper H. *Epilepsy and the Functional Anatomy of the Human Brain*. London, England: Churchill; 1954.
18. Button J, Putnam T. Visual responses to cortical stimulation in the blind. *J Iowa St Med Soc* 1962;52:17-21.
19. Brindley GS, Lewin WS. The sensations produced by electrical stimulation of the visual cortex. *J Physiol* 1968;196:479-493.
20. Brindley G, Rushton D. Implanted stimulators of the visual cortex as visual prosthetic devices. *TransAm Acad Ophthalmol Otolaryngol* 1974;78:OP-741-OP-745.
21. Pollen DA. Responses of single neurons to electrical stimulation of the surface of the visual cortex. *Brain Behav Evol* 1977;14:67-86.
23. Dobelle WH, Mladejovsky MG. Phosphenes produced by electrical stimulation of human occipital cortex, and their application to the development of a prosthesis for the blind. *J Physiol* 1974;243:553-576.
24. Karny H. Clinical and physiological aspects of the cortical visual prosthesis. *Surv Ophthalmol* 1975;20:47-58.
25. Bak M, Girvin JP, Hambrecht FT, et al . Visual sensations produced by intracortical microstimulation of the human occipital cortex. *Med Biol Eng Comput* 1990;28:257-259.
26. Dobelle WH, Mladejovsky MG, Evans JR, et al. "Braille" reading by a blind volunteer by visual cortex stimulation. *Nature* 1976;259:111-112
27. Evans JR, Gordon J, Abramov I, et al. Brightness of phosphenes elicited by electrical stimulation of human visual cortex. *Sens Processes* 1979;3:82-94.

Mark, Thesis 11/9/01 11:29 AM Page 297




28. Girvin JP, Evans JR, Dobelle WH, et al. Electrical stimulation of human visual cortex: The effect of stimulus parameters on phosphene threshold. *Sens Processes* 1979;3:66-81.
29. Henderson DC, Evans JR, Dobelle WH. The relationship between stimulus parameters and phosphene threshold/brightness, during stimulation of human visual cortex. *Trans Am Soc Artif Intern Organs* 1979;25:367-371.
30. Dobelle WH. Artificial vision for the blind by connecting a television camera to the visual cortex. *Am Soc Artific Internal Organs J* 2000;46:3-9.
31. Uematsu S, Chapanis N, Gucer G, et al. Electrical stimulation of the cerebral visual system in man. *Confin Neurol* 1974;36:113-124.
32. Schmidt EM, Bak MJ, Hambrecht FT, et al. Feasibility of a visual prosthesis for the blind based on intracortical microstimulation of the visual cortex. *Brain* 1996;119 (platinum 2):507-522.
33. Normann RA, Maynard EM, Rousche PJ, et al. A neural interface for a cortical vision prothesis. *Vision Res* 1999;39:2577-2587.
34. Jones KE, Normann RA. An advanced demultiplexing system for physiological stimulation. *IEEE Trans Biomed Eng* 1997;44:1210-1220.
35. Maynard EM, Nordhausen CT, Normann RA. The Utah intracortical Electrode Array: A recording structure for potential brain-computer interfaces. *Electroencephalogr Clin Neurophysiol* 1997;102:228-239.
36. Nordhausen CT, Maynard EM, Normann RA. Single unit recording capabilities of a 100 microelectrode array. *Brain Res* 1996;726:129-140.
37. Potts AM, Inoue J., Buffum D. The electrically evoked response of the visual system (EER). *Invest Ophthalmol* 1968;7:269-278.
38. Potts A.M., Inoue J. The electrically evoked response (EER) of the visual system II. Effect of adaptation and retinitis pigmentosa. *Invest Ophthalmol* 1969;8:605-612.
39. Potts AM, Inoue J. The electrically evoked response of the visual system (EER) III. Further consideration to the origin of the EER. *Invest Ophthalmol* 1970;9:814-819.
40. Stone JL, Barlow WE, Humayun MS, et al. Morphometric analysis of macular photoreceptors and ganglion cells in retinas with retinitis pigmentosa. *Arch Ophthalmol* 1992;110:1634-1639.
41. Santos A, Humayun MS, de Juan EJ, et al. Preservation of the inner retina in retinitis pigmentosa. A morphometric analysis. *Arch Ophthalmol* 1997;115:511-515.
42. Humayun MS, Prince M, de Juan EJ, et al. Morphometric analysis of the extramacular retina from postmortem eyes with retinitis pigmentosa. *Invest Ophthalmol Vis Sci* 1999;40:143-148.
43. Curcio CA, Medeiros NE, Millican CL. Photoreceptor loss in age-related macular degeneration. *Invest Ophthalmol Vis Sci* 1996;37:1236-1249.
44. Kim S, Sadda S, Pearlman J, et al. Morphometric analysis of the macula in eyes with disciform age-related macular degeneration. *Arch Ophthalmol* (Submitted).
45. Dawson WW, Radtke ND. The electrical stimulation of the retina by indwelling electrodes. *Invest Ophthalmol Vis Sci* 1977;16:249-252.
46. Humayun M, Propst R, de Juan EJ, et al. Bipolar surface electrical stimulation of the vertebrate retina. *Arch Ophthalmol* 1994;112:110-116.
47. Humayun MS, de Juan EJ, Weiland JD, et al. Pattern electrical stimulation of the human retina. *Vision Res* 1999;39:2569-2576.
48. Zrenner E, Stett A, Weiss S, et al. Can subretinal microphotodiodes successfully replace degenerated photoreceptors? *Vision Res* 1999;39:2555-2567.
49. Chow AY, Peachey NS. The subretinal microphotodiode array retinal prosthesis. (Letter and Comment) *Ophthalmic Res* 1998;30:195-198.
50. Eckmiller R. Learning retina implants with epiretinal contacts. *Ophthalmic Res* 1997;29:281-289.
51. Wyatt J., Rizzo JF. Ocular Implants for the blind. *IEEE Spectrum* 1996;112:47-53.
52. Veraart C, Raftopoulos C, Mortimer JT, et al. Visual sensations produced by optic nerve stimulation using an implanted self-sizing spiral cuff electrode. *Brain Res* 1998;813:181-186.
53. Yagi T, Hayashida Y. Implantation of the artificial retina. *Nippon Rinsho* 1999;57:1208-1215.
54. Humayun MS, de Juan EJ, Dagnelie G, et al. Visual perception elicited by electrical stimulation of retina in blind humans. *Arch Ophthalmol* 1996;114:40-46.
55. Suzuki, S, Humayun, MS, de Juan E, et al. A comparison of electrical stimulation threshold in normal mouse retina vs different aged retinal degenerate (rd) mouse retina. *Annual meeting of the Association for Research in Vision and Ophthalmology*, 1999, Fort Lauderdale, Fla. Abstract 3886.S735.
56. Chen SJ, Humayun MS, Weiland JD. Electrical stimulation of the mouse retina: A study of electrically elicited visual cortical responses. *Annual Meeting of the Association for Research in Vision and Ophthalmology*, 1999, Fort Lauderdale, Fla. Abstract 3886.S735.
57. Weiland JD, Humayun MS, Suzuki S, et al. Electrically evoked response (EER) from the visual cortex in normal and retinal degenerate dog. *Annual Meeting of the Association for Research in Vision and Ophthalmology*, 1999, Fort Lauderdale, Fla. Abstract 4125.S783
58. Rizzo J, Wyatt J, Loewenstein J, et al. Acute intraocular retinal stimulation in normal and blind humans. *Annual Meeting of the Association for Research in Vision and Ophthalmology*, 2000, Fort Lauderdale, Fla. Abstract 532.S102
59. Majji AB, Humayun MS, Weiland JD, et al. Long-term histological and electrophysiological results of an inactive epiretinal electrode array implantation in dogs. *Invest Ophthalmol Vis Sci* 1999;40:2073-2081.
60. Rizzo J, Wyatt J. Prospects for a visual prosthesis. *Neuroscientist* 1997;3:251-262.
61. Monroe R. Pigmentosa patients get retina on a chip. EyeNet 2000;4(8):14.
62. Tassicker. US patent 2760483. 1956.
63. Chow AY, Chow VY. Subretinal electrical stimulation of the rabbit retina. *Neurosci Lett* 1997;225:13-16.
64. Peyman G, Chow AY, Liang C, et ak . Subretinal semiconductor microphotodiode array. *Ophthalmic Surg Lasers* 1998;29:234-241.
65. Guenther E, Troger B, Schlosshauer B, et al. Long-term survival of retinal cell cultures on retinal implant materials. *Vision Res* 1999;39:3988-3994.
66. Shandurina AN. Restoration of visual and auditory function using electrostimulation. *Fiziol Cheloveka* 1995;21:25-29.
67. Shandurina AN, Panin AV, Sologubova EK, et al. Results of the use of therapeutic periorbital electrostimulation in neurological patients with partial atrophy of the optic nerves. *Neurosci Behav Physiol* 1996;26:137-142.
68. Yagi T, Watanabe M. A computational study on an electrode array in a hybrid retinal implant. *Proc 1998 IEEE Int Joint Conf Neural Networks* 1998;780-783.
69. Brabyn JA. New developments in mobility and orientation aids for the blind. *IEEE Trans Biomed Eng* 1982;29:285-289.
70. Rita P, Kaczmarek KA, Tyler ME, et al. Form perception with a 49-point electrotactile stimulus array on the tongue: a technical note. *J Rehabil Res Dev* 1998;35:427-430.
71. Rocha G, Baines MG, Deschenes J. The immunology of the eye and its systemic interactions. *Crit Rev Immunol* 1992;12:81-100.
72. Scheinberg LC, Levy A, Edelman F. Is the brain an "immunologically privileged site"? 2. Studies in induced host resistance to transplantable mouse glioma following irradiation of prior implants. *Arch Neurol* 1965;13:283-286.
73. Oehmichen M. Inflammatory cells in the central nervous system: an integrating concept based on recent research in pathology, immunology and forensic medicine. *Prog Neuropath* 1983;5:277-335.

Mark, Thesis 11/9/01 11:29 AM Page 298




74. Dougherty SH, Simmons RL. Infections in bionic man: The pathobiology of infections in prosthetic devices-Part II. *Curr Probl Surg* 1982;19:265-319.
75. Walter P, Szurman P, Vobig M, et al . Successful long-term implantation of electrically inactive epiretinal microelectrode arrays in rabbits. *Retina* 1999;19:546-552.
76. Veraart C, Grill WM, Mortimer JT. Selective control of muscle activation with a multipolar nerve cuff electrode. *IEEE Trans Biomed Eng* 1993;40:640-653.
77. Rousche PJ, Normann RA. A method for pneumatically inserting an array of penetrating electrodes into cortical tissue. *Ann Biomed Eng* 1992;20:413-422.
78. Margalit E, Fujii G, Lai J, et al. Bioadhesives for intraocular use. *Retina* 2000;20:469-477.
79. Lowenstein J, Rizzo JF, Shahin M, et al. Novel retinal adhesive used to attach electrode array to retina. *Annual Meeting of the Association for Research in Vision and Ophthalmology*, 1999, Fort Lauderdale, Fla. Abstract 3874.
80. Harpster T, Hauvespre S, Dokmecy M, et al. A passive humidity monitoring system for in-situ remote wireless testing of micropackages. *13th Annual Internetaional Conference on Microelectromechanical Systems* 2000;335-340.
81. Wise KD, Najafi K. Microfabrication techniques for integrated sensors and microsystems. *Science* 1991;254:1335-1342.
82. Von Arx J, Ziaie B, Dokmeci M, et al. Hermeticity testing of glass-silicon packages with on-chip feedthroughs. *8th International Conference on Solid-state Sensors and Actuators*. 1995;244-247.
83. Cheng YT, Lin L, Najafi K. Fabrication and hermeticity testing of a glass-silicon package formed using localized aluminum/silicon-to-glass bonding. *13th Annual International Conference on Microelectromechanical Systems*. 2000;757-762.
84. Pudenz RH, Bullara LA, Jacques S, et al. Electrical stimulation of the brain. III. The neural damage model. *Surg Neurol* 1975;4:389-400.
85. Pudenz RH, Bullara LA, Dru D, et al. Electrical stimulation of the brain. II. Effects on the blood-brain barrier. *Surg Neurol* 1975;4:265-270.
86. Pudenz RH, Bullara LA, Talalla A. Electrical stimulation of the brain. I. Electrodes and electrode arrays. *Surg Neurol* 1975;4:37-42.
87. Brummer SB, Turner M.J. Electrical stimulation of the nervous system: The principle of safe charge injection with noble metal electrodes. Bioelectrochem *Bioenerget* 1975;2:13-25.
88. Lilly JC. Injury and excitation by electric currents: The balanced pulse-pair waveform. In: Sheer DE, ed. *Electrical Stimulation of the Brain*. Hogg Foundation for Mental Health; 1961.
89. Bard AJ, Faulkner LR. *Electrochemical Methods: Fundamentals and Applications*. New York, NY: John Wiley & Sons; 1980;213-248.
90. McCreery DB, Agnew WF, Yuen TG, et al. Comparison of neural damage induced by electrical stimulation with faradic and capacitor electrodes. *Ann Biomed Eng* 1988;16:463-481.
91. McCreery DB, Agnew WF, Yuen TGH, et al. Charge density and charge per phase as cofactors in neural injury induced by electrical stimulation. *IEEE Trans Biomed Eng* 1990;37:996-1001.
92. McCreery DB, Yuen TG, Agnew WF, et al. A characterization of the effects on neuronal excitability due to prolonged microstimulation with chronically implanted microelectrodes. *IEEE Trans Biomed Eng* 1997;44:931-939.
93. Brown WJ, Babb TL, Soper HV, et al. Tissue reactions to long-term electrical stimulation of the cerebellum in monkeys. *J Neurosurg* 1977;47:366-379.
94. Tehovnik E. Electrical stimulation of neural tissue to evoke behavioral responses. *J Neurosci Methods* 1996;65:1-17.
95. Agnew WF, Yuen TGH, McCreery DB, et al. Histopathologic evaluation of prolonged intracortical electrical stimulation. *Exp Neurol* 1986;92:162-185.
96. Weiland JD, Anderson DJ. Chronic neural stimulation with thin-film, iridium oxide stimulating electrodes. *IEEE Trans Biomed Eng* 2000;47:911-918.
97. Bullara LA, McCreery DB, Yuen TG, et al. A microelectrode for delivery of defined charge densities. *J Neurosci Methods* 1983;9:15-21.
98. Clark GM. Electrical stimulation of the auditory nerve: The coding of frequency, the perception of pitch and the development of cochlear implant speech processing strategies for profoundly deaf people. *Clin Exp Pharmacol Physiol* 1996;23:766-776.
99. Grill WM, Mortimer JT. Stability of the input-output properties of chronically implanted multiple contact nerve cuff stimulating electrodes. *IEEE Trans Rehabil Eng* 1998;6:364-373.
100. McCreery DB, Bullara L, Agnew WF. Neuronal activity evoked by chronically implanted intracortical microelectrodes. *Exp Neurol* 1986;92:147-161.
101. McCreery D, Agnew W. Mechanisms of stimulation-induced neural damage and their relation to guidelines for safe stimulation. In: Agnew W, McCreery D, eds. *Neural Prostheses Fundamental Studies*. Englewood Cliffs, NJ: Prentice Hall; 1990;297-317.
102. Riu PJ, Foster KR. Heating of tissue by near-field exposure to a dipole: A model analysis. *IEEE Trans Biomed Eng* 1999;46:911-917.
103. Piyathaisere DV, Margalit E, Chen SJ, et al. Effects of short-term exposure to heat on the retina. Annual Meeting of the Association for Research in Vision and Ophthalmology, 2001, Fort Lauderdale, Fla (Submitted).
104. Ko WH, Liang SP, Fung CD. Design of radio-frequency powered coils for implant instruments. *Med Biol Eng Comput* 1977;15:634-640.
105. Heetderks WJ. RF powering of millimeter and submillimeter sized neural prosthetic implants. *IEEE Trans Biomed Eng* 1988;35:323-326.
106. Liu W, Vichienchom K, Clements M, et al. A neuro-stimulus chip with telemetry unit for retinal prosthesis device. *IEEE Solid-State Circuits* 2000;35:1487-1497.
107. Zrenner E, Miliczek KD, Gabel VP, et al. The development of subretinal microphotodiodes for replacement of degenerated photoreceptors. *Ophthalmic Res* 1997;29:269-280.
108. Marshall S, Skitek G. *Electromagnetic Concepts and Applications*. 2nd ed. Englewood Cliffs, NJ: Prentice-Hall; 1987.
109. Schubert M, Hierzenberger A, Lehner H, et al. Optimizing photodiodes arrays for the use as retinal implants. *Sensors Actuators* 1999;74:193-197.
110. Brummer SB, Robblee LS, Hambrecht FT. Criteria for selecting electrodes for electrical stimulation: theoretical and practical considerations. *Ann N Y Acad Sci* 1983;405:159-171.
111. McHardy J, Robblee LS, Marston JM, et al. Electrical stimulation with platinum electrodes. IV. Factors influencing platinum dissolution in inorganic saline. *Biomaterials* 1980;1:129-134.
112. Robblee LS, McHardy J, Marston JM, et al. Electrical stimulation with platinum electrodes. V. The effect of protein on platinum dissolution. *Biomaterials* 1980;1:135-139.
113. Beebe X, Rose TL. Charge injection limits of activated iridium oxide electrodes with 0.2 ms pulses in bicarbonate buffered saline. *IEEE Trans Biomed Eng* 1988;35:494-495.
114. Janders M, Egert U, Stelze M, et al. Novel thin-film titanium nitride micro-electrodes with excellent charge transfer capability for cell Stimulation and sensing applications. *Proc 19th Int Conf IEEE/EMBS* 1996;1191-1193.
115. Greenberg RJ. *Analysis of Electrical Stimulation of the Vertebrate Retina: Work Towards a Retinal Prosthesis* (Dissertation). Baltimore, Md: Johns Hopkins University; 1998.
116. Rose TL, Kelliher EM, Robblee LS. Assessment of capacitor electrodes for intracortical neural stimulation. *J Neurosci Methods* 1985;12:181-193.
117. Wiley JD, Webster JG. Analysis and control of the current distribution under circular dispersive electrodes. *IEEE Trans Biomed Eng* 1982;29:381-385.

Mark, Thesis 11/9/01 11:29 AM Page 299




118. Rubinstein JT, Spelman FA, Soma M, et al. Current density profiles of surface mounted and recessed electrodes for neural prostheses. *IEEE Trans Biomed Eng* 1987;34:864-875.
119. Grill WM, Mortimer JT. Electrical properties of implant encapsulation tissue. *Ann Biomed Eng* 1994;22:23-33.
120. Wise KD, Angell J, Starr A. An integrated-circuit approach to extracellular microelectrodes. *IEEE Trans Biomed Eng* 1970;BME-17:238-247.
121. Hetke JF, Lund JL, Najafi K, et al. Silicon ribbon cables for chronically implantable microelectrode arrays. *IEEE Trans Biomed Eng* 1994;41:314-321.
122. BeMent SL, Wise KD, Anderson DJ, et al. Solid-state electrodes for multichannel multiplexed intracortical neuronal recording. *IEEE Trans Biomed Eng* 1986;33:230-241.
123. Kovacs GT, Storment CW, Rosen JM. Regeneration microelectrode array for peripheral nerve recording and stimulation. *IEEE Trans Biomed Eng* 1992;39:893-902.
124. Turner JN, Shain W, Szarowski DH, et al. Cerebral astrocyte response to micromachined silicon implants. *Exp Neurol* 1999;156:33-49.
125. Anderson DJ, Najafi K, Tanghe SJ, et al. Batch-fabricated thin-film electrodes for stimulation of the central auditory system. *IEEE Trans Biomed Eng* 1989;36:693-704.
126. Najafi K, Hetke JF. Strength characterization of silicon microprobes in neurophysiological tissues. *IEEE Trans Biomed Eng* 1990;37:474-481.
127. Tanghe S, Wise K. A 16-channel CMOS neural stimulating array. *IEEE Solid-State Circuits* 1992;27:1819-1825.
128. Jones KE, Campbell PK, Normann RA. A glass/silicon composite intracortical electrode array. *Ann Biomed Eng* 1992;20:423-437.
129. Cole K, Curtis H. Electric impedance of the squid giant axon during activity. *J Gen Physiol* 1939;22:649-670.
130. Hodgkin A, Huxley A. A quantitative description of membrane current and its application to conduction and excitation in nerve. *J Physiol* 1952;117:500-544.
131. Hodgkin A, Huxley A. Currents carried by sodium and potassium ions through the membrane of the giant axon of loligo. *J Physiol* 1952;116:472-449.
132. Knighton RW. An electrically evoked slow potential of the frog's retina. I. Properties of response. *J Neurophysiol* 1975;38:185-197.
133. Dowling J. The Retina: *An Approachable Part of the Brain*. London, England: Belknap Press of Harvard University Press; 1987.
134. Greenberg RJ, Velte TJ, Humayun MS, et al. A computational model of electrical stimulation of the retinal ganglion cell. *IEEE Trans Biomed Eng* 1999;46:505-514.
135. Ranck JB Jr. Which elements are excited in electrical stimulation of mammalian central nervous system: A review. *Brain Res* 1975;98:417-440.
136. Shepherd RK, Hatsushika S, Clark GM. Electrical stimulation of the auditory nerve: The effect of electrode position on neural excitation. *Hear Res* 1993;66:108-120.
137. Szlavik RB, de Bruin H. The effect of anisotropy on the potential distribution in biological tissue and its impact on nerve excitation simulations. *IEEE Trans Biomed Eng* 2000;47:1202-1210.
138. West DC, Wolstencroft JH. Strength-duration characteristics of myelinated and non-myelinated bulbospinal axons in the cat spinal cord. *J Physiol* 1983;337:37-50.
139. Grill WM Jr, Mortimer JT. The effect of stimulus pulse duration on selectivity of neural stimulation. *IEEE Trans Biomed Eng* 1996;43:161-166.
140. Bostock H. The strength-duration relationship for excitation of myelinated nerve: Computed dependence on membrane parameters. *J Physiol* 1983;341:59-74.
141. Gorman PH, Mortimer JT. The effect of stimulus parameters on the recruitment characteristics of direct nerve stimulation. *IEEE Trans Biomed Eng* 1983;30:407-414.
142. Robblee LS, Mangaudis MJ, Lasinski ED, et al. Charge injection properties of thermally-prepared iridium oxide films. *Matls Res Soc Symp Proc* 1986;55:303-310.
143. Bartlett JR, Doty RW. An exploration of the ability of macaques to detect microstimulation of striate cortex. *Acta Neurobiol Exp* 1980;40:713-727.
144. Shyu, JS, Maia, M, Weiland, JD, et al. *Electrical Stimulation of Isolated Rabbit Retina*. Presented at the Annual Meeting of the Biomedical Engineering Society, Seattle, Wash, 2000.
145. Grumet AE, Wyatt JL, Rizzo JF. Multi-electrode stimulation and recording in the isolated retina. *J Neurosci Methods* 2000;101:31-42.
146. Stett A, Barth W, Weiss S, et al. Electrical multisite stimulation of the isolated chicken retina. *Vision Res* 2000;40:1785-1795.
147. Hesse L, Schanze T, Wilms M, et al. Implantation of retina stimulation electrodes and recording of electrical stimulation responses in the visual cortex of the cat. *Graefes Arch Clin Exp Ophthalmol* 2000;238:840-845.
148. Grumet AE, Rizzo JF, Wyatt JL. Ten micron diameter electrodes directly stimulate rabbit retinal ganglion cell axons. *Annual Meeting of the Association for Research in Vision and Ophthalmology*, 1999, Fort Lauderdale, Fla. Abstract 3883.
149. Grumet AE, Rizzo JF, Wyatt J. In-vitro electrical stimulation of human retinal ganglion cell axons. *Annual Meeting of the Association for Research in Vision and Ophthalmology*, 2000, Fort Lauderdale, Fla. Abstract 50.
150. Stett A, Tepfenhart M, Kohler K, et al. Charge sensitivity of electrically stimulated chicken and RCS rat retinae. *Annual Meeting of the Association for Research in Vision and Ophthalmology*, 1999, Fort Lauderdale, Fla. Abstract 3892.
151. Shimazu K, Miyake Y, Fukatsu Y, et al. Striate cortical contribution to the transcorneal electrically evoked response of the visual system. *Jpn J Ophthalmol* 1996;40:469-479.
152. Margalit E, Weiland JD, Clatterbuck R, et al. Light and electrically evoked response (VER, EER) recorded from sub-dural epileptic electrodes implanted above the visual cortex in normal dogs. *Annual Meeting of the Association for Research in Vision and Ophthalmology*, 2001, Fort Lauderdale, Fla (Submitted).
153. Weiland JD, Humayun MS, Dagnelie G, et al. Understanding the origin of visual percepts elicited by electrical stimulation of the human retina. *Graefes Arch Clin Exp Ophthalmol* 1999;237:1007-1013.
154. Knighton RW. An electrically evoked slow potential of the frog's retina. II. Identification with PII component of electroretinogram. *J Neurophysiol* 1975;38:198-209.
155. Brindley GS. The number of information channels needed for efficient reading. *J Physiol* 1965;177:44-44P.
156. Sterling TD, Vaughn HG Jr. Feasibility of electrocortical prosthesis. In: Sterling TD, ed. *Visual Prosthesis: The Interdisciplinary Dialogue*. New York: Academic Press; 1971:1-17.
157. Cha K, Horch KW, Normann RA. Mobility performance with a pixelized vision system. *Vision Res* 1992;32:1367-1372.
158. Cha K, Horch KW, Normann RA, et al. Reading speed with a pixelized vision system. *J Opt Soc Am* 1992;9:673-677.
159. Cha K, Horch K, Normann RA. Simulation of a phosphene-based visual field: Visual acuity in a pixelized vision system. *Ann Biomed Eng* 1992;20:439-449.
160. Liu W, McGucken E, Clemments M, et al. The engineering of a retinal implant. *Annual Meeting of the Association for Research in Vision and Ophthalmology*, 1999, Fort Lauderdale, Fla. Abstract 4120.
161. Liu W, McGucken E, Vitchiccom K, et al. Dual unit visual intraocular prosthesis. *19th International Conference of the IEEE/EMBS*, 1997, Chicago, Ill. 2303-2306.

Mark, Thesis 11/9/01 11:29 AM Page 300



**SELECTED READINGS**


- Dobelle WH. Artificial vision for the blind. The summit may be closer than you think. *ASAIO J* 1994;40:919-922.
- Garcia-Fernandez JM, Jimenez AJ, Foster RG. The persistence of cone photoreceptors within the dorsal retina of aged retinally degenerate mice (rd/rd): Implications for circadian organization. *Neurosci Lett* 1995;187:33-36.
- Ogilvie JM, Tenkova T, Lett JM, et al. Age-related distribution of cones and ON-bipolar cells in the rd mouse retina. *Curr Eye Res* 1997;16:244-251.
- Rose TL, Robblee LS. Electrical stimulation with platinum electrodes. VIII. Electrochemically safe charge injection limits with 0.2 ms pulses. *IEEE Trans Biomed Eng* 1990;37:1118-1120.
- Sanyal S, Zeilmaker GH. Development and degeneration of retina in rds mutant mice: light and electron microscopic observations in experimental chimaeras. *Exp Eye Res* 1984;39:231-246.
- Sato S, Sugimoto S, Chiba S. A procedure for recording electroretinogram and visual evoked potential in conscious dog. *J Pharmacol Methods* 1982;8:173-181.
- Shimazu K, Miyake Y, Watanabe S. Retinal ganglion cell response properties in the transcorneal electrically evoked response of the visual system. *Vision Res* 1999;39:2251-2260.
- Toyoda J, Fujimoto M. Application of transretinal current stimulation for the study of bipolar-amacrine transmission. *J Gen Physiol* 1984;84:915-925.
- Troyk P, Schwan M. Closed-loop class E transcutaneous power and data link for microimplants. *IEEE Trans Biomed Eng* 1992;39:589-599.